An efficient iterative method for solving multiple scattering in locally inhomogeneous media

Ziqing Xie[a], Rui Zhang[a], Bo Wang[a,*], Li-Lian Wang[b]

[a] *LCSM(MOE), School of Mathematics and Statistics, Hunan Normal University, Changsha, Hunan, 410081, PR China*
[b] *Division of Mathematical Sciences, School of Physical and Mathematical Sciences, Nanyang Technological University, 637371, Singapore*

Highlights

- An efficient iterative method is proposed for solving multiple scattering problem in locally inhomogeneous media.
- At each iteration, only single scattering problems need to be solved. An effective way is introduced to handle the communication between scatterers.
- The convergence of the iterative method is proved by using the compactness of involved integral operators.

Abstract

In this paper, an efficient iterative method is proposed for solving multiple scattering problem in locally inhomogeneous media. The key idea is to enclose the inhomogeneity of the media by well separated artificial boundaries and then apply purely outgoing wave decomposition for the scattering field outside the enclosed region. As a result, the original multiple scattering problem can be decomposed into a finite number of single scattering problems, where each of them communicates with the other scattering problems only through its surrounding artificial boundary. Accordingly, they can be solved in a parallel manner at each iteration. This framework enjoys a great flexibility in using different combinations of iterative algorithms and single scattering problem solvers. The spectral element method seamlessly integrated with the non-reflecting boundary condition and the GMRES iteration is advocated and implemented in this work. The convergence of the proposed method is proved by using the compactness of involved integral operators. Ample numerical examples are presented to show its high accuracy and efficiency.

1. Introduction

The acquaintance of many physical phenomena and engineering processes can be significantly enhanced by accurately simulating the multiple scattering problems involving configurations of many obstacles. Typically, for
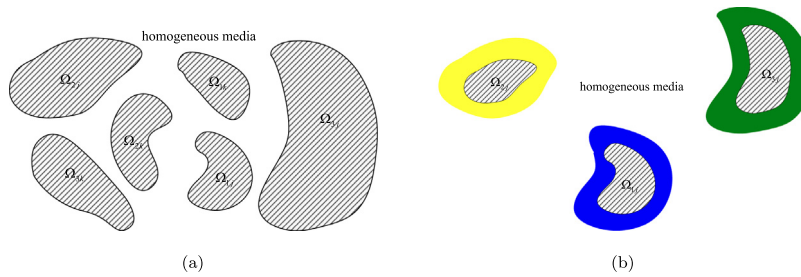

Fig. 1.1. Configurations of multiple scattering. (a): Scatterers embedded in homogeneous media; (b): Well-separated scatterers with inhomogeneous media in colored area. (For interpretation of the references to color in this figure legend, the reader is referred to the web version of this article.)

two-dimensional time-harmonic acoustic multiple scattering in inhomogeneous media, we consider the Helmholtz equation of the form

$$\Delta u(\boldsymbol{x}) + \kappa^2 n^2(\boldsymbol{x}) u(\boldsymbol{x}) = 0, \quad \text{in } \mathbb{R}^2 \setminus \Omega, \tag{1.1}$$

where $u = u^{\mathrm{sc}} + u^{\mathrm{in}}$ is the total field, κ is the wave number, $n^2(\boldsymbol{x})$ is the index of refraction, Ω is a region occupied by M impenetrable scatterers in $\mathbb{R}^2$, see Fig. 1.1. The scattering field u^{sc} satisfies the Sommerfeld radiation condition

$$\frac{\partial u^{\mathrm{sc}}}{\partial r} - \mathrm{i}\kappa u^{\mathrm{sc}} = o(r^{-1/2}), \quad \text{as } r := |\boldsymbol{x}| \to \infty. \tag{1.2}$$

On the boundaries of the scatterers, the Dirichlet, Neumann or Robin boundary conditions can be imposed according to different materials of the scatterers. Here, let M_1, M_2, M_3 be the number of scatterers with Dirichlet, Neumann and Robin boundary conditions, respectively, and denote by Ω_{1j}, Ω_{2j}, Ω_{3j} the jth scatterer in each group. Accordingly, we denote the domain of all obstacles and its boundary by

$$\Omega = \Omega_1 \cup \Omega_2 \cup \Omega_3, \quad \partial\Omega = \partial\Omega_1 \cup \partial\Omega_2 \cup \partial\Omega_3 \quad \text{with} \quad \Omega_i = \bigcup_{j=1}^{M_i} \Omega_{ij}, \tag{1.3}$$

for $i = 1, 2, 3$ corresponding to the Dirichlet, Neumann and Robin boundary conditions, respectively. For notational convenience, we express these three types of boundary conditions on the scatterers as

$$\mathscr{B}_i u = 0, \quad \boldsymbol{x} \in \partial\Omega_i, \quad i = 1, 2, 3, \tag{1.4}$$

where

$$\mathscr{B}_1 = \mathcal{I}, \quad \mathscr{B}_2 = \frac{\partial}{\partial \boldsymbol{n}}, \quad \mathscr{B}_3 = \frac{\partial}{\partial \boldsymbol{n}} + h\mathcal{I}. \tag{1.5}$$

Here, $\mathcal{I}$ is the identity operator, $\boldsymbol{n}$ is the unit outward normal on $\partial\Omega_2$ and h is a given function defined on $\partial\Omega_3$.

It is known that analytic solutions for wave scattering problems from multiple arbitrary shaped obstacles embedded in inhomogeneous media are not available. Partially for this reason, many early works are mostly restricted to cylindrical and spherical obstacles embedded in homogeneous media, where the modal expansions of the scattered fields play an essential role (cf. [1–5]). We highlight that the reader-friendly monograph by Martin [6] was largely concerned with time-harmonic waves with multiple obstacles and with exact methods including separation of variables, integral equations and T-matrices, but only the last chapter is concerned with some numerics.

Among limited works for multiple scattering problems with general bounded scatterers (compared with intensive studies of single scattering problems), the boundary integral method is one of the methods of choice. By reformulating a scattering problem into an integral equation on the boundary of scatterers (cf. [7–9]), numerical methods (e.g., boundary element methods) have been developed based on the Galerkin or collocation formulations (cf. [10,11]). Very recently, the boundary integral method with fast multipole acceleration and hybrid numerical-asymptotic boundary element method have been investigated for relatively low frequency (cf. [12]) and high frequency problems (cf. [13,14]), respectively. However, it is noteworthy that the boundary integral method relies

on the Green's function to derive integral equation on the boundary, which in general is not applicable to inhomogeneous media.

In analogue with solving general single scattering problems, one can reduce the unbounded domain by a proper domain truncation technique, before applying a finite-domain solver, e.g., the finite element method. Grote and Kirsch [15] proposed the non-reflecting boundary conditions (NRBC) based on Dirichlet-to-Neumann operators for truncating multiple time-harmonic acoustic scattering problems with well-separated scatterers in two dimensions, where each scatterer is surrounded by an NRBC. The framework therein is well-suited for numerical discretization, but it requires to solve coupled systems. Indeed, Acosta and Villamizar [16,17] discussed the multiple acoustic scattering from scatterers of complex shape using coupling of Dirichlet-to-Neumann boundary condition and the finite difference method. In practice, the iterative method is more desirable. Based on the decomposition of the scattering wave into purely outgoing waves, Neumann iterative method was proposed in [18], where at each iteration, only single scattering problems need to be solved. This iterative technique has been further developed for high frequency problems with a large number of scatterers, see [11,19–22] and the references therein. Recently, a block Gauss–Seidel iterative method was employed to solve the linear systems resulted from the finite element discretization (cf. [23–25]). Error estimates between the iterative scheme at continuous level and its finite element discretization was analyzed in [24]. Most of the aforementioned works are for homogeneous media.

In this paper, we propose an efficient iterative method for solving multiple scattering problem in locally inhomogeneous media, and show the convergence of the method. The algorithm consists of three components. Firstly, the scatterers and inhomogeneity of the media are enclosed by well-separated artificial boundaries such that purely outgoing wave decomposition is applicable outside the enclosed domains. Then the scattering field is decomposed into purely outgoing waves and boundary integral equations with respect to density functions on the artificial boundaries are formulated. Secondly, we change the unknowns in the resulted boundary integral equations by using solution operators of the interior and exterior problems. New equations using the value of purely outgoing fields and total field on the artificial boundaries as unknowns can be derived. Thirdly, the iterative methodology (e.g., Gauss–Seidel, general minimum residue) is applied.

The proposed method enjoys the advantage that only the interior problems (together with analytic formulas for solutions of exterior problems) with respect to single scatterer need to be solved separately at each iteration. Various single scattering problem solvers and iterative methods can be applied. Thus, this approach possesses excellent flexibility and high parallelizability. In this work, the high order spectral element method with non-reflecting boundary condition (NRBC) and GMRES iterative method is adopted. We remark that other numerical PDE solvers (e.g., finite element method or finite difference method) can also be used for solving single scattering problems. Here, we basically solve a boundary integral equation on the artificial boundaries. The convergence of the method can be proved by using the compactness of involved integral operators. Moreover, the well-conditioning feature of the boundary integral equation leads to a small number of iterations for convergence. This is the main difference between our method and the Neumann iterative method. Numerical results show that the number of iterations is nearly independent of the mesh size and polynomial degree used in the discretization. This paper will focus on two dimensional scenarios, but the proposed method is extendable to three dimensional cases.

Note that the final discrete systems resulted from the discretization proposed by [15–17] have block structure, so the block iterative methods can be directly applied (e.g., block Gauss–Seidel iterative method [23,24]). Although the pursuit of "decoupling" between scatterers is similar to these works, the derivation of our iterative algorithm is from the boundary integral equations that leads to more effective communication between scatterers. Moreover, this allows us to conduct the convergence analysis based on the tools in the boundary integral equations. Indeed, the numerical comparisons show that such a treatment of the interactions between scatterers is more effective than the existing approaches in particular for a large number of scatterers. This also can relax the assumption of the well separateness of the scatterers when the problems in homogeneous media are tackled.

The rest of this paper is organized as follows. In Section 2, we use the multiple scattering problem in homogeneous media to illustrate the main idea of the iterative method. By using the classic potential theory, the boundary integral equations with respect to purely outgoing fields are derived for three typical boundary conditions. Then the iterative algorithm using GMRES iteration is presented. In Section 3, the iterative method in locally inhomogeneous media is proposed. We first introduce artificial boundaries to enclose the inhomogeneity of the media and then show that an outgoing wave decomposition can be used to derive equations with respect to outgoing fields and total field on the artificial boundaries. Iterative method together with spectral element discretization is

proposed for the coupled equations. In Section 4, we give theoretical proof for the convergence of the iterative method by using the compactness of the involved integral operators. Various numerical examples are presented in Section 5. By comparing with a direct spectral element discretization to the truncation using one sufficiently large artificial boundary to enclose all scatterers inside, we validate the effectiveness of our method. The more efficient communication strategy between scatterers is also validated by numerical comparisons with the approach in [15].

2. Iterative method for multiple scattering in homogeneous media

In this section, we focus on the multiple scattering problem in homogeneous media, i.e., $n(\boldsymbol{x}) \equiv 1$ in (1.1), and propose an iterative method based on the boundary integral equations on the scatterers. As we shall see in the next section, this actually paves the way for the algorithm and analysis of the multiple scattering in locally inhomogeneous media, where the boundary integral formulations on the artificial boundaries can be seamlessly integrated with the interior solver for each single scatterer. In particular, due to the circular artificial boundaries, the integral operators related to the single scattering problems (3.2) can be solved analytically, so the boundary integral operators are only used in the derivation and the convergence analysis.

2.1. Integral equations on the boundaries of the scatterers

Given a generic bounded domain $D \subset \mathbb{R}^2$ and a density function $\phi \in L^2(\partial D)$, the corresponding single-layer and double-layer potentials are defined as (cf. [7,26]):

$$\mathcal{S}\phi(\boldsymbol{x}) := \int_{\partial D} G_\kappa(\boldsymbol{x}, \boldsymbol{y})\phi(\boldsymbol{y})\,\mathrm{d}\boldsymbol{y}, \quad \mathcal{D}\phi(\boldsymbol{x}) := \int_{\partial D} \frac{\partial G_\kappa(\boldsymbol{x}, \boldsymbol{y})}{\partial \boldsymbol{n}(\boldsymbol{y})}\phi(\boldsymbol{y})\,\mathrm{d}S_{\boldsymbol{y}}, \quad \boldsymbol{x} \notin \partial D, \tag{2.1}$$

where

$$G_\kappa(\boldsymbol{x}, \boldsymbol{y}) = -\frac{\mathrm{i}}{4} H_0^{(1)}(\kappa|\boldsymbol{x} - \boldsymbol{y}|), \tag{2.2}$$

is the Green's function in free space. For any function $v(\boldsymbol{x})$, we distinguish its limit values obtained by approaching the boundary ∂D from inside $\mathbb{R}^2 \setminus \bar{D}$ and D, respectively, by

$$v^+(\boldsymbol{x}) = \lim_{\substack{\boldsymbol{y} \to \boldsymbol{x} \\ \boldsymbol{y} \notin D}} v(\boldsymbol{y}), \quad v^-(\boldsymbol{x}) = \lim_{\substack{\boldsymbol{y} \to \boldsymbol{x} \\ \boldsymbol{y} \in D}} v(\boldsymbol{y}), \quad \boldsymbol{x} \in \partial D. \tag{2.3}$$

Similarly, we denote the limit values of the normal derivative at $\boldsymbol{x} \in \partial D$ from two sides by

$$\partial_n^+ v(\boldsymbol{x}) := \lim_{\substack{\boldsymbol{y} \to \boldsymbol{x} \\ \boldsymbol{y} \notin D}} \nabla v(\boldsymbol{y}) \cdot \boldsymbol{n}_{\boldsymbol{x}}, \quad \partial_n^- v(\boldsymbol{x}) := \lim_{\substack{\boldsymbol{y} \to \boldsymbol{x} \\ \boldsymbol{y} \in D}} \nabla u(\boldsymbol{y}) \cdot \boldsymbol{n}_{\boldsymbol{x}}, \quad \boldsymbol{x} \in \partial D. \tag{2.4}$$

Although the Green's function is singular as $\boldsymbol{x} \to \boldsymbol{y}$, the limits of $\mathcal{S}\phi(\boldsymbol{x}), \mathcal{D}\phi(\boldsymbol{x})$ as $\boldsymbol{x}$ approach ∂D remain finite and well-defined. Indeed, in electrostatics, they represent a physical potential and an electric field generated by finite charge or dipole densities. According to the potential theory (cf. [7,27]), they are given by the following Cauchy principle value (p.v.) and Hadamard finite part (p.f.).

Proposition 2.1. *The single layer potential $\mathcal{S}\phi(\boldsymbol{x})$ is continuous across the boundary ∂D, and*

$$\mathcal{S}\phi(\boldsymbol{x}) = \mathrm{p.v.} \int_{\partial D} G_\kappa(\boldsymbol{x}, \boldsymbol{y})\phi(\boldsymbol{y})\mathrm{d}S_{\boldsymbol{y}}, \quad \boldsymbol{x} \in \partial D, \tag{2.5}$$

while $\frac{\partial \mathcal{S}\phi(\boldsymbol{x})}{\partial \boldsymbol{n}}$ has a jump, namely

$$\partial_n^\pm \mathcal{S}\phi(\boldsymbol{x}) = \mathrm{p.v.} \int_{\partial D} \frac{\partial G_\kappa(\boldsymbol{x}, \boldsymbol{y})}{\partial \boldsymbol{n}(\boldsymbol{x})}\phi(\boldsymbol{y})\mathrm{d}S_{\boldsymbol{y}} \mp \frac{\phi(\boldsymbol{x})}{2}, \quad \boldsymbol{x} \in \partial D, \tag{2.6}$$

which implies

$$[\![\partial_n \mathcal{S}\phi(\boldsymbol{x})]\!] := \partial_n^+ \mathcal{S}\phi(\boldsymbol{x}) - \partial_n^- \mathcal{S}\phi(\boldsymbol{x}) = -\phi(\boldsymbol{x}), \quad \boldsymbol{x} \in \partial D. \tag{2.7}$$

Proposition 2.2. *The double layer potential $\mathcal{D}\phi(\boldsymbol{x})$ is discontinuous across ∂D, and there holds*

$$(\mathcal{D}\phi(\boldsymbol{x}))^\pm = \mathrm{p.v.} \int_{\partial D} \frac{\partial G_\kappa(\boldsymbol{x}, \boldsymbol{y})}{\partial \boldsymbol{n}(\boldsymbol{y})}\phi(\boldsymbol{y})\mathrm{d}S_{\boldsymbol{y}} \pm \frac{\phi(\boldsymbol{x})}{2}, \quad \boldsymbol{x} \in \partial D, \tag{2.8}$$

and

$$\llbracket \mathcal{D}\phi(\boldsymbol{x}) \rrbracket := (\mathcal{D}\phi(\boldsymbol{x}))^+ - (\mathcal{D}\phi(\boldsymbol{x}))^- = \phi(\boldsymbol{x}), \quad \boldsymbol{x} \in \partial D. \tag{2.9}$$

Meanwhile, the normal derivative of the double layer potential is continuous across ∂D and

$$\partial_{\boldsymbol{n}}\mathcal{D}\phi(\boldsymbol{x}) = \text{p.f.} \int_{\partial D} \frac{\partial^2 G_\kappa(\boldsymbol{x},\boldsymbol{y})}{\partial \boldsymbol{n}(\boldsymbol{x})\partial \boldsymbol{n}(\boldsymbol{y})}\phi(\boldsymbol{y})\mathrm{d}S_{\boldsymbol{y}}, \quad \boldsymbol{x} \in \partial D. \tag{2.10}$$

The potential theory introduced above can be directly used to derive boundary integral equations for multiple scattering problem in homogeneous media. However, it will lead to a very large linear system when a large number of scatterers are involved. To overcome this, we formulate the boundary integral equations based on the decomposed form derived from the superposition principle. It is known that the scattering field u^{sc} of the multiple scattering problem (1.1)–(1.4) in homogeneous media has the following unique decomposition (cf. [28]):

$$u^{\text{sc}}(\boldsymbol{x}) = \sum_{j=1}^{M_1} w_{1j}(\boldsymbol{x}) + \sum_{j=1}^{M_2} w_{2j}(\boldsymbol{x}) + \sum_{j=1}^{M_3} w_{3j}(\boldsymbol{x}), \tag{2.11}$$

where w_{ij} are the solutions of the single scattering problems

$$\begin{cases} \Delta w_{ij} + \kappa^2 w_{ij} = 0, & \text{in} \quad \Omega_{ij}^\infty := \mathbb{R}^2 \setminus \bar{\Omega}_{ij}, & \text{(a)} \\ \mathcal{B}_{ij} w_{ij} = g_{ij}, & \text{on} \quad \partial \Omega_{ij}, & \text{(b)} \\ \frac{\partial w_{ij}}{\partial \boldsymbol{n}} - \mathrm{i}k w_{ij} = o(r^{-\frac{1}{2}}), & \text{as} \quad r := |\boldsymbol{x}| \to \infty, & \text{(c)} \end{cases} \tag{2.12}$$

for $j = 1, \ldots, M_i$, $i = 1, 2, 3$. The input data is given by

$$g_{ij} = -\mathcal{B}_{ij}u^{\text{in}} - \sum_{k=1,k\neq j}^{M_i} \mathcal{B}_{ij}w_{ik} - \sum_{\ell=1,\ell\neq i}^{3} \sum_{k=1}^{M_\ell} \mathcal{B}_{ij}w_{\ell k}. \tag{2.13}$$

The last two terms in (2.13) involve the scattering fields from all other scatterers. It is seen that due to the interaction between the scatterers, the incident wave g_{ij} for the jth scatterer in the ith group is the combination of u^{in} and the scattering fields generated by all other scatterers. This shows how the multiple scattering system is coupled.

According to the potential theory, the single and double-layer potentials defined by (2.1) satisfy the Helmholtz equation in $\mathbb{R}^2 \setminus \partial D$ and the Sommerfeld radiation condition at infinity. For the uniqueness of the resulted boundary integral equations, we define the mixed potentials (cf. [7,8]):

$$\mathcal{K}_{1j}\phi_{1j} := \mathcal{D}_{1j}\phi_{1j} + \mathrm{i}\eta\mathcal{S}_{1j}\phi_{1j}, \quad \mathcal{K}_{ij}\phi_{ij} := -\mathrm{i}\eta\mathcal{D}_{ij}\phi_{ij} - \mathcal{S}_{ij}\phi_{ij}, \quad i = 2, 3, \tag{2.14}$$

for the densities $\{\phi_{1j}, \phi_{2j}, \phi_{3j}\}$, where

$$\mathcal{S}_{ij}\phi_{ij} := \int_{\partial \Omega_{ij}} G_\kappa(\boldsymbol{x},\boldsymbol{y})\phi_{ij}(\boldsymbol{y})\mathrm{d}\boldsymbol{y}, \quad \mathcal{D}_{ij}\phi_{ij}(\boldsymbol{x}) := \int_{\partial \Omega_{ij}} \frac{\partial G_\kappa(\boldsymbol{x},\boldsymbol{y})}{\partial \boldsymbol{n}(\boldsymbol{y})}\phi_{ij}(\boldsymbol{y})\mathrm{d}S_{\boldsymbol{y}}, \quad \forall \boldsymbol{x} \notin \partial \Omega_{ij},$$

are single and double layer potentials on $\partial \Omega_{ij}$, and η is a given constant satisfying $\eta\mathfrak{Re}\kappa \geq 0$. Then the solutions of single scattering problems (2.12)(a)–(c) have the form

$$w_{ij}(\boldsymbol{x}) = \mathcal{K}_{ij}\phi_{ij}(\boldsymbol{x}), \quad \boldsymbol{x} \notin \partial \Omega_{ij}, \tag{2.15}$$

while the density functions $\{\phi_{ij}\}$ satisfy boundary integral equations:

$$\frac{1}{2}\phi_{ij} + \widehat{\mathcal{K}_{ij}}\phi_{ij} = g_{ij}, \quad \boldsymbol{x} \in \partial \Omega_{ij}, \ j = 1, 2, \ldots, M_i, \ i = 1, 2, 3. \tag{2.16}$$

The boundary integral operators $\widehat{\mathcal{K}_{ij}}$ are defined as

$$\widehat{\mathcal{K}_{1j}} := \widehat{\mathcal{D}}_{1j} + \mathrm{i}\eta\widehat{\mathcal{S}}_{1j}, \quad \widehat{\mathcal{K}_{2j}} := -\mathrm{i}\eta\widehat{\mathcal{D}}_{2j} - \widehat{\mathcal{S}}_{2j}, \quad \widehat{\mathcal{K}_{3j}} := -\mathrm{i}\eta\widehat{\mathcal{D}}_{3j} - \widehat{\mathcal{S}}_{3j} - \frac{\mathrm{i}}{2}\eta h, \tag{2.17}$$

where

$$\widehat{\mathcal{S}}_{1j}\phi_{1j}(\boldsymbol{x}) := \text{p.v.} \int_{\partial\Omega_{1j}} G_\kappa(\boldsymbol{x}, \boldsymbol{y})\phi_{1j}(\boldsymbol{y})\mathrm{d}S_{\boldsymbol{y}}, \quad \widehat{\mathcal{D}}_{1j}\phi_{1j}(\boldsymbol{x}) := \text{p.v.} \int_{\partial\Omega_{1j}} \frac{\partial G_\kappa(\boldsymbol{x}, \boldsymbol{y})}{\partial\boldsymbol{n}(\boldsymbol{y})}\phi_{1j}(\boldsymbol{y})\mathrm{d}S_{\boldsymbol{y}},$$

$$\widehat{\mathcal{S}}_{2j}\phi_{2j}(\boldsymbol{x}) := \text{p.v.} \int_{\partial\Omega_{2j}} \frac{\partial G_\kappa(\boldsymbol{x}, \boldsymbol{y})}{\partial\boldsymbol{n}(\boldsymbol{x})}\phi_{2j}(\boldsymbol{y})\mathrm{d}S_{\boldsymbol{y}}, \quad \widehat{\mathcal{D}}_{2j}\phi_{2j}(\boldsymbol{x}) := \text{p.f.} \int_{\partial\Omega_{2j}} \frac{\partial^2 G_\kappa(\boldsymbol{x}, \boldsymbol{y})}{\partial\boldsymbol{n}(\boldsymbol{x})\partial\boldsymbol{n}(\boldsymbol{y})}\phi_{2j}(\boldsymbol{y})\mathrm{d}S_{\boldsymbol{y}},$$

$$\widehat{\mathcal{S}}_{3j}\phi_{3j}(\boldsymbol{x}) := h\Big(\text{p.v.} \int_{\partial\Omega_{3j}} G_\kappa(\boldsymbol{x}, \boldsymbol{y})\phi_{3j}(\boldsymbol{y})\mathrm{d}S_{\boldsymbol{y}}\Big) + \text{p.v.} \int_{\partial\Omega_{3j}} \frac{\partial G_\kappa(\boldsymbol{x}, \boldsymbol{y})}{\partial\boldsymbol{n}(\boldsymbol{x})}\phi_{3j}(\boldsymbol{y})\mathrm{d}S_{\boldsymbol{y}},$$

$$\widehat{\mathcal{D}}_{3j}\phi_{3j}(\boldsymbol{x}) := h\Big(\text{p.v.} \int_{\partial\Omega_{3j}} \frac{\partial G_\kappa(\boldsymbol{x}, \boldsymbol{y})}{\partial\boldsymbol{n}(\boldsymbol{y})}\phi_{3j}(\boldsymbol{y})\mathrm{d}S_{\boldsymbol{y}}\Big) + \text{p.f.} \int_{\partial\Omega_{3j}} \frac{\partial^2 G_\kappa(\boldsymbol{x}, \boldsymbol{y})}{\partial\boldsymbol{n}(\boldsymbol{x})\partial\boldsymbol{n}(\boldsymbol{y})}\phi_{3j}(\boldsymbol{y})\mathrm{d}S_{\boldsymbol{y}}.$$

Applying the integral representations (2.15) to (2.13) gives

$$g_{ij}(\boldsymbol{x}) = -\mathcal{B}_{ij}u^{\text{in}}(\boldsymbol{x}) - \sum_{k=1, k\neq j}^{M_i} \mathcal{B}_{ij}\mathcal{K}_{ik}\phi_{ik}(\boldsymbol{x}) - \sum_{\ell=1, \ell\neq i}^{3}\sum_{k=1}^{M_\ell} \mathcal{B}_{ij}\mathcal{K}_{\ell k}\phi_{\ell k}(\boldsymbol{x}), \quad \forall \boldsymbol{x} \in \partial\Omega_{ij}. \tag{2.18}$$

Then, substituting (2.18) into (2.16) leads to the following system of boundary integral equations, which is uniquely solvable (cf. [7]).

Proposition 2.3. *The boundary integral equations of the problem* (2.12)–(2.13) *take the form:*

$$\frac{1}{2}\phi_{ij} + \widehat{\mathcal{K}_{ij}}\phi_{ij} + \sum_{k=1, k\neq j}^{M_i} \mathcal{B}_{ij}\mathcal{K}_{ik}\phi_{ik} + \sum_{\ell=1, \ell\neq i}^{3}\sum_{k=1}^{M_\ell} \mathcal{B}_{ij}\mathcal{K}_{\ell k}\phi_{\ell k} = -\mathcal{B}_{ij}u^{\text{in}}, \tag{2.19}$$

for all $\boldsymbol{x} \in \partial\Omega_{ij}$, $j = 1, 2, \ldots, M_i$, $i = 1, 2, 3$. *The scattering field* u^{sc} *can be obtained by using* (2.11) *and* (2.15).

2.2. Iterative method

Recall that w_{ij} and ϕ_{ij} are, respectively, the solution and the density of the scattering problem (2.12), so we have

$$\Big(\frac{1}{2}\mathcal{I} + \widehat{\mathcal{K}_{ij}}\Big)\phi_{ij} = W_{ij} := \mathcal{B}_{ij}w_{ij}, \quad \text{on } \partial\Omega_{ij}. \tag{2.20}$$

According to the boundary integral equation theory (cf. [7]), the operator $\widetilde{\mathcal{K}_{ij}} := \frac{1}{2}\mathcal{I} + \widehat{\mathcal{K}_{ij}}$ is invertible and its inverse is bounded. Substituting $\phi_{ij} = \widetilde{\mathcal{K}_{ij}}^{-1}W_{ij}$ into (2.19), leads to

$$W_{ij} + \sum_{k=1, k\neq j}^{M_i} \mathcal{B}_{ij}\mathcal{K}_{ik}\widetilde{\mathcal{K}_{ik}}^{-1}W_{ik} + \sum_{\ell=1, \ell\neq i}^{3}\sum_{k=1}^{M_\ell} \mathcal{B}_{ij}\mathcal{K}_{\ell k}\widetilde{\mathcal{K}_{\ell k}}^{-1}W_{\ell k} = -\mathcal{B}_{ij}u^{\text{in}}, \quad \text{on } \partial\Omega_{ij}. \tag{2.21}$$

Let $\mathcal{S}_{ij} : C(\partial\Omega_{ij}) \mapsto C^2(\mathbb{R}^2 \setminus \overline{\Omega}_{ij})$ be the solution operator of the single scattering problem

$$\begin{cases} \Delta v + \kappa^2 v = 0, & \boldsymbol{x} \in \mathbb{R}^2 \setminus \overline{\Omega}_{ij}, \\ \mathcal{B}_{ij}v = \psi, & \boldsymbol{x} \in \partial\Omega_{ij}, \\ \dfrac{\partial v}{\partial r} - \mathrm{i}\kappa v = o\big(r^{-\frac{1}{2}}\big), & \text{as } r := |\boldsymbol{x}| \to \infty. \end{cases} \tag{2.22}$$

We find readily from (2.15)–(2.16) and (2.22) (with $\psi = g_{ij}$) that

$$\mathcal{K}_{ij}\widetilde{\mathcal{K}_{ij}}^{-1} = \mathcal{S}_{ij}. \tag{2.23}$$

Thus, the operators $\mathcal{K}_{ij}\widetilde{\mathcal{K}_{ij}}^{-1}$ in (2.21) can be replaced by the solution operator $\mathcal{S}_{ij}$. As a result, we have the following system

$$(\mathcal{I} + \mathbb{K})\boldsymbol{W} = \boldsymbol{b}, \tag{2.24}$$

where $\boldsymbol{W} = (W_{11}, \ldots, W_{1M_1}, W_{21}, \ldots, W_{2M_2}, W_{31}, \ldots, W_{3M_3})^{\mathrm{T}}$, and

$$
\mathbb{K} = \begin{pmatrix} \mathcal{O} & \mathcal{B}_{11} & \cdots & \mathcal{B}_{11} \\ \mathcal{B}_{12} & \mathcal{O} & \cdots & \mathcal{B}_{12} \\ \vdots & \vdots & \ddots & \vdots \\ \mathcal{B}_{3M_3} & \mathcal{B}_{3M_3} & \cdots & \mathcal{O} \end{pmatrix} \begin{pmatrix} \mathcal{S}_{11} & \mathcal{O} & \cdots & \mathcal{O} \\ \mathcal{O} & \mathcal{S}_{12} & \cdots & \mathcal{O} \\ \vdots & \vdots & \ddots & \vdots \\ \mathcal{O} & \mathcal{O} & \cdots & \mathcal{S}_{3M_3} \end{pmatrix}.
\tag{2.25}
$$

Different from the classic boundary integral method, which usually solves (2.19) for the density, we use an iterative method to solve (2.24)–(2.25) with different unknowns (note: it is equivalent to the integral equation (2.21)). In fact, many iterative approaches (e.g., Gauss–Seidel or generalized minimal residue) can be employed. For the sake of convergence analysis, we choose the generalized minimal residual (GMRES cf. [29]) iterative method (see Algorithm 1).

As we have seen in the proposed iterative algorithm, the key part in GMRES iteration is the computation of the terms $\mathcal{S}_{ij} W_{ij}^{(k)}$ in $(\mathcal{I} + \mathbb{K})\boldsymbol{W}^{(k)}$, where $W_{ij}^{(k)}$ is given boundary data. Here, we will apply the spectral element solver with NRBC truncation to the single scattering problems in (2.22). We first truncate the unbounded computational domain $\mathbb{R}^2 \setminus \Omega_{ij}$ by using a circular artificial boundary namely Γ^{ij} centered at $\boldsymbol{c}_{ij} = (x_{ij}^c, y_{ij}^c)$ with radius R_{ij} (see Fig. 2.1). Denote by B_{ij} the domain enclosed by Γ^{ij}. Then the scattering problem (2.22) can be reduced to the following boundary value problems (BVPs):

$$
\begin{cases} \Delta v + \kappa^2 v = 0, & \boldsymbol{x} \in B_{ij} \setminus \Omega_{ij}, \\ \mathcal{B}_{ij} v = \psi & \boldsymbol{x} \in \partial \Omega_{ij}, \\ \partial_{\boldsymbol{n}} v = \mathcal{T}_{ij} v, & \boldsymbol{x} \in \Gamma^{ij}, \end{cases}
\tag{2.26}
$$

Algorithm 1 Iterative algorithm for multiple scattering in homogeneous media

---

Initialization

(i) Given $\boldsymbol{W}^{(0)}$ on the boundary of $\{\Omega_{ij}\}$, stopping threshold: ε and the maximum number of iterations: n_{max};

(ii) Solve (2.22) with $\psi = W_{ij}^{(0)}$ for $w_{ij}^{(0)} = \mathcal{S}_{ij} W_{ij}^{(0)}$, $i = 1, 2, 3$, $j = 1, 2, \cdots, M_i$;

(iii) Compute $\boldsymbol{r}^{(0)} = \boldsymbol{b} - (\mathcal{I} + \mathbb{K})\boldsymbol{W}^{(0)}$, and $\boldsymbol{v}^{(1)} = \boldsymbol{r}^{(0)}/\|\boldsymbol{r}^{(0)}\|$.

Iterative steps

for $n = 1, 2, \cdots, n_{max}$ **do**
    for $k = 2 \to n$ **do**
        Solve (2.22) with $\psi = v_{ij}^{(k-1)}$ for $\tilde{v}_{ij} = \mathcal{S}_{ij} v_{ij}^{(k-1)}$, $i = 1, 2, 3$, $j = 1, 2, \cdots, M_i$;
        Compute $\boldsymbol{v}^{(k)} = (\mathcal{I} + \mathbb{K})\boldsymbol{v}^{(k-1)}$;
        for $m = 1 \to k - 1$ **do**

$$
h_{m,k-1} = (\boldsymbol{v}^{(m)}, \boldsymbol{v}^{(k)}); \quad \boldsymbol{v}^{(k)} = \boldsymbol{v}^{(k)} - h_{m,k-1}\boldsymbol{v}^{(m)};
\tag{2.27}
$$

        end for
        $h_{k,k-1} = \|\boldsymbol{v}^{(k)}\|$, $\boldsymbol{v}^{(k)} = \boldsymbol{v}^{(k)}/h_{k,k-1}$;
    end for
    Compute $\boldsymbol{W}^{(n)} = W^0 + \sum_{i=1}^{n-1} y_i \boldsymbol{v}_i$, where $\boldsymbol{y} = (y_1, y_2, \cdots, y_{n-1})^{\mathrm{T}}$ minimizes

$$
J(\boldsymbol{y}) := \|(\|\boldsymbol{r}_0\|\boldsymbol{e}_1) - \bar{H}_{n-1}\boldsymbol{y}\|.
\tag{2.28}
$$

    if $J(\boldsymbol{y}) \leq \varepsilon$ **then**
        Stop iteration.
    end if
end for

Final step

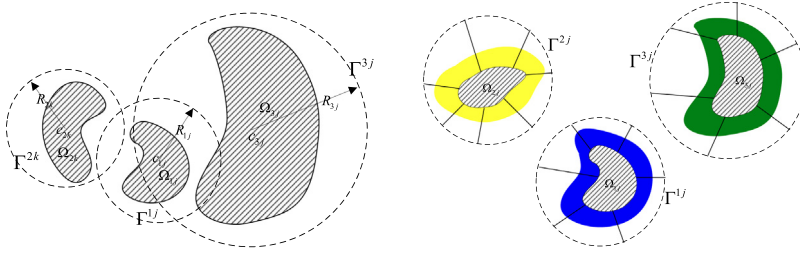Solve (2.22) with $\psi = W_{ij}^{(n)}$ for $w_{ij}^{(n)}$, $j = 1, 2, \cdots, M_i$, $i = 1, 2, 3$.

Fig. 2.1. Left: Intersecting artificial boundaries. Right: Well-separated artificial boundaries and spectral element mesh for inhomogeneous media problem.

where the DtN operators in the NRBC are given by

$$\mathscr{T}_{ij}v := \sum_{n=-\infty}^{\infty} \kappa \frac{H_n^{(1)'}(\kappa R_{ij})}{H_n^{(1)}(\kappa R_{ij})} \widehat{v}_n e^{\mathrm{i}n\theta_{ij}}. \tag{2.29}$$

Here, (r_{ij}, θ_{ij}) are the polar coordinates of $\boldsymbol{x} - \boldsymbol{c}_{ij}$, $\{H_n^{(1)}(z)\}$ are the Hankel functions of the first kind, and

$$\widehat{v}_n = \frac{1}{2\pi} \int_0^{2\pi} v(x_{ij}^c + R_{ij}\cos\theta_{ij}, y_{ij}^c + R_{ij}\sin\theta_{ij})e^{\mathrm{i}n\theta_{ij}} \mathrm{d}\theta_{ij}, \tag{2.30}$$

are the Fourier coefficients of v on the artificial boundary Γ^{ij}. The scattering fields outside the truncated domains will be calculated from the data along the artificial boundaries by using the separation of variable method. More details on the discretization will be provided in the next section.

Remark 2.1. Artificial boundaries in other forms (e.g., ellipse) can also be used in (2.26) for better adaptation to the shapes of the scatterers. Different from the well separated artificial boundaries required by the DtN boundary condition proposed in [15], the artificial boundaries Γ^{ij} used here are independent of each other. They are used individually in the truncation of each single scattering problem (2.22). Therefore overlapped artificial boundaries can be used as shown in Fig. 2.1 (Left). This can relax the assumption of the well separateness of the scatterers.

Although the essential unknowns are the boundary data W_{ij} on $\partial\Omega_{ij}$, the purely outgoing components w_{ij} in the exterior domains $\mathbb{R}^2 \setminus \overline{\Omega}_{ij}$ will be calculated in the iterations. According to the algorithm, only M single scattering problems need to be solved individually at each iteration. Since the system (2.21) is an equivalent form of the boundary integral system (2.19), it enjoys the nice property of relatively small condition number. Consequently, the proposed iterative method converges within a small number of iterations. It will be validated by the numerical examples in Section 5 that the number of iterations is nearly independent of the mesh size and polynomial degree used in the discretization.

3. Iterative method for the multiple scattering in locally inhomogeneous media

In this section, we present the iterative method for multiple scattering problems in locally inhomogeneous media. In general, purely outgoing wave decomposition is not available when inhomogeneous medium is involved. Nevertheless, it is usually reasonable to assume that the inhomogeneity of the medium is confined in a finite domain [15].

3.1. Integral equations on the artificial boundaries

Assuming that all scatterers are well separated, we can surround them by M non-intersecting circles $\{\Gamma^{ij}\}_{j=1}^{M_i}$, $i = 1, 2, 3$ centered at $\{\boldsymbol{c}_{ij} = (x_{ij}^c, y_{ij}^c)\}$ with radii R_{ij} (see Fig. 2.1). Denote by B_{ij} the domain enclosed by Γ^{ij}, $B_i = \cup_{j=1}^{M_i} B_{ij}$ and $B = B_1 \cup B_2 \cup B_3$. We further assume that $1 - n(\boldsymbol{x})$ vanishes outside the finite region B, i.e., the inhomogeneity is confined inside B (see Fig. 2.1 (right)). A medium under this assumption is called a

locally inhomogeneous medium. As such, the medium outside the region B is homogeneous, and the scattering field $u^{\mathrm{sc}} = u - u^{\mathrm{in}}$ outside B has a unique decomposition (cf. [15,28]):

$$u^{\mathrm{sc}}(\boldsymbol{x}) = \sum_{j=1}^{M_1} w_{1j}(\boldsymbol{x}) + \sum_{j=1}^{M_2} w_{2j}(\boldsymbol{x}) + \sum_{j=1}^{M_3} w_{3j}(\boldsymbol{x}), \quad \boldsymbol{x} \in \mathbb{R}^2 \setminus \bar{B}, \tag{3.1}$$

where $\{w_{ij}\}_{j=1}^{M_i}$ are the solutions of the scattering problems:

$$\begin{cases} \Delta w_{ij} + \kappa^2 w_{ij} = 0, & \text{in} \quad \mathbb{R}^2 \setminus \bar{B}_{ij}, \\ w_{ij} = g_{ij}, & \text{on} \quad \Gamma^{ij}, \\ \dfrac{\partial w_{ij}}{\partial r} - \mathrm{i}\kappa w_{ij} = o\!\left(r^{-\frac{1}{2}}\right), & \text{as} \quad r := |\boldsymbol{x}| \to \infty, \end{cases} \tag{3.2}$$

for $j = 1, \ldots, M_i$, $i = 1, 2, 3$. The boundary data $\{g_{ij}\}$ are

$$g_{ij} = u - u^{\mathrm{in}} - \sum_{k=1, k \neq j}^{M_i} w_{ik} - \sum_{\ell=1, \ell \neq i}^{3} \sum_{k=1}^{M_\ell} w_{\ell k}, \quad \text{on} \quad \Gamma^{ij}. \tag{3.3}$$

It is worthy pointing out that we have used the total field u to determine g_{ij}. For notational convenience, we define

$$\widetilde{\mathscr{T}}_{ij} : C(\Gamma_{ij}) \mapsto C^2(\mathbb{R}^2 \setminus \overline{B}_{ij}) \tag{3.4}$$

as the solution operator of the exterior problem (3.2).

Remark 3.1. In the model problem, the inhomogeneity of the medium is assumed to be in the neighborhood of each scatterer and well-separated. If the inhomogeneity around some scatterers is not well-separated, these scatterers should be treated as a group surrounded by a relatively larger artificial boundary.

As in (2.14), we define the mixed potentials $\mathscr{K}'_{ij}\phi_{ij} = \mathcal{D}'_{ij}\phi_{ij} + \mathrm{i}\eta \mathcal{S}'_{ij}\phi_{ij}$ with the densities ϕ_{ij}, where $\mathcal{S}'_{ij}\phi_{ij}$, $\mathcal{D}'_{ij}\phi_{ij}$ are single and double layer potentials on Γ^{ij}, and η is a given constant such that $\eta \mathfrak{Re}\kappa \geq 0$. According to the boundary integral theory, the solutions of the local scattering problems (3.2) have the following integral representations:

$$w_{ij}(\boldsymbol{x}) = \mathscr{K}'_{ij}\phi_{ij}(\boldsymbol{x}), \quad \forall \boldsymbol{x} \in \mathbb{R}^2 \setminus \bar{B}_{ij}, \tag{3.5}$$

where the density functions $\{\phi_{ij}\}$ satisfy the boundary integral equations

$$\widehat{\mathscr{K}'_{ij}}\phi_{ij} + \frac{1}{2}\phi_{ij} = g_{ij}, \quad \boldsymbol{x} \in \Gamma^{ij}, \quad j = 1, 2, \ldots, M_i, \quad i = 1, 2, 3, \tag{3.6}$$

with the boundary integral operators given by

$$\widehat{\mathscr{K}'_{ij}}\phi_{ij} = \mathrm{i}\eta \, \mathrm{p.v.} \int_{\Gamma^{ij}} G_\kappa(\boldsymbol{x}, \boldsymbol{y}) \phi_{ij}(\boldsymbol{y}) \, \mathrm{d}S_{\boldsymbol{y}} + \mathrm{p.v.} \int_{\Gamma^{ij}} \frac{\partial G_\kappa(\boldsymbol{x}, \boldsymbol{y})}{\partial \boldsymbol{n}(\boldsymbol{y})} \phi_{ij}(\boldsymbol{y}) \mathrm{d}S_{\boldsymbol{y}}. \tag{3.7}$$

Boundary integral equations (3.6) are derived by applying the Dirichlet boundary conditions in (3.2) and the limiting properties given in Propositions 2.1 and 2.2. Then substituting (3.5) into (3.3), gives

$$g_{ij} = u - u^{\mathrm{in}} - \sum_{k=1, k \neq j}^{M_i} \mathscr{K}'_{ik}\phi_{ik} - \sum_{\ell=1, \ell \neq i}^{3} \sum_{k=1}^{M_\ell} \mathscr{K}'_{\ell k}\phi_{\ell k}, \quad \text{on} \quad \Gamma^{ij}, \tag{3.8}$$

As a direct consequence of (3.6) and (3.8), we have the following system of integral equations:

$$\frac{1}{2}\phi_{ij} + \widehat{\mathscr{K}'_{ij}}\phi_{ij} + \sum_{k=1, k \neq j}^{M_i} \mathscr{K}'_{ik}\phi_{ik} + \sum_{\ell=1, \ell \neq i}^{3} \sum_{k=1}^{M_\ell} \mathscr{K}'_{\ell k}\phi_{\ell k} - u = -u^{\mathrm{in}}, \quad \text{on} \quad \Gamma^{ij}, \tag{3.9}$$

for $j = 1, 2, \ldots, M_i$, $i = 1, 2, 3$.

3.2. Iterative method

It is seen that Eq. (3.9) involves the total field u restricted to the artificial boundaries Γ^{ij}. Nevertheless, they can be determined by the densities $\{\phi_{ij}\}_{j=1}^{M_i}$, $i = 1, 2, 3$ via solving the boundary value problems in $B_{ij} \setminus \overline{\Omega}_{ij}$, respectively. To show this, let

$$\mathscr{S}_{ij}' : H^{-\frac{1}{2}}(\Gamma_{ij}) \mapsto H^1(B_{ij} \setminus \overline{\Omega}_{ij}), \tag{3.10}$$

be the solution operator of the inhomogeneous interior problem

$$\begin{cases} \Delta v(\boldsymbol{x}) + \kappa^2 n(\boldsymbol{x}) v(\boldsymbol{x}) = 0, & \boldsymbol{x} \in B_{ij} \setminus \overline{\Omega}_{ij}, \\ \mathscr{B}_{ij} v = 0, & \boldsymbol{x} \in \partial \Omega_{ij}, \\ \mathscr{T}_{ij}' v = \mathscr{T}_{ij}' u^{\mathrm{in}} + \psi, & \boldsymbol{x} \in \Gamma^{ij}, \end{cases} \tag{3.11}$$

where $\mathscr{T}_{ij}' := \frac{\partial}{\partial \boldsymbol{n}} - \mathscr{T}_{ij}$, and $\mathscr{T}_{ij}$ is the DtN operator defined in (2.29). Recall that by the decomposition (3.1), the total field on Γ^{ij} has the decomposition:

$$u(\boldsymbol{x}) = u^{\mathrm{in}}(\boldsymbol{x}) + \sum_{\ell=1}^{3} \sum_{k=1}^{M_\ell} w_{\ell k}(\boldsymbol{x}), \quad \boldsymbol{x} \in \Gamma^{ij}. \tag{3.12}$$

Moreover, the purely outgoing wave w_{ij} satisfies the boundary condition $\mathscr{T}_{ij}' w_{ij}(\boldsymbol{x}) = 0$ for all $\boldsymbol{x} \in \Gamma^{ij}$. Then, from (3.12), we have

$$\mathscr{T}_{ij}' u = \mathscr{T}_{ij}' \Big(u^{\mathrm{in}} + \sum_{k=1, k \neq j}^{M_i} w_{ik} + \sum_{\ell=1, \ell \neq i}^{3} \sum_{k=1}^{M_\ell} w_{\ell k} \Big), \quad \boldsymbol{x} \in \Gamma^{ij}, \tag{3.13}$$

which implies that u in the domain $\bar{B}_{ij} \setminus \Omega_{ij}$ is the solution of (3.11) with the boundary data

$$\psi = \mathscr{T}_{ij}' \Big(\sum_{k=1, k \neq j}^{M_i} w_{ik} + \sum_{\ell=1, \ell \neq i}^{3} \sum_{k=1}^{M_\ell} w_{\ell k} \Big). \tag{3.14}$$

The following classical result ensures the well-posedness of the BVP (3.11) (cf. [30]).

Theorem 3.1. *Let Ω_{ij} be a Lipschitz domain, $n(\boldsymbol{x}) \in L^\infty(B_{ij} \setminus \overline{\Omega}_{ij})$, $\psi \in H^{-\frac{1}{2}}(\Gamma^{ij})$. Then (3.11) has a unique weak solution in $H^1(B_{ij} \setminus \overline{\Omega}_{ij})$ such that*

$$\|v\|_{H^1(B_{ij} \setminus \overline{\Omega}_{ij})} \leq C \|\psi\|_{H^{-\frac{1}{2}}(\Gamma^{ij})}. \tag{3.15}$$

In view of (3.5) and (3.14), the total field u in $\bar{B}_{ij} \setminus \Omega_{ij}$ can be represented by the solution operator $\mathscr{S}_{ij}'$ as

$$u(\boldsymbol{x}) = \mathscr{S}_{ij}' \mathscr{T}_{ij}' \Big(\sum_{k=1, k \neq j}^{M_i} \mathscr{K}_{ik}' \phi_{ik} + \sum_{\ell=1, \ell \neq i}^{3} \sum_{k=1}^{M_\ell} \mathscr{K}_{\ell k}' \phi_{\ell k} \Big), \quad \boldsymbol{x} \in \bar{B}_{ij} \setminus \Omega_{ij}. \tag{3.16}$$

Substituting it into (3.9), we obtain the equations:

$$\frac{1}{2}\phi_{ij} + \widehat{\mathscr{K}_{ij}'} \phi_{ij} + (\mathcal{I} - \mathscr{S}_{ij}' \mathscr{T}_{ij}') \Big(\sum_{k=1, k \neq j}^{M_i} \mathscr{K}_{ik}' \phi_{ik} + \sum_{\ell=1, \ell \neq i}^{3} \sum_{k=1}^{M_\ell} \mathscr{K}_{\ell k}' \phi_{\ell k} \Big) = -u^{\mathrm{in}}, \quad \text{on } \Gamma^{ij}. \tag{3.17}$$

Recall that w_{ij} and ϕ_{ij} are the scattering fields and the corresponding densities of the single scattering problems (3.2). Then

$$\Big(\frac{1}{2}\mathcal{I} + \widehat{\mathscr{K}_{ij}'} \Big) \phi_{ij} = W_{ij} := w_{ij}\big|_{\Gamma^{ij}}. \tag{3.18}$$

Again the boundary integral equation theory (cf. [7]) implies that the operator $\widetilde{\mathcal{K}}'_{ij} := \frac{1}{2}\mathcal{I} + \widehat{\mathcal{K}'_{ij}}$ is invertible and its inverse is a bounded linear operator. Substituting $\phi_{ij} = \widetilde{\mathcal{K}}'^{-1}_{ij} W_{ij}$ into (3.17), leads to

$$W_{ij} + (\mathcal{I} - \mathcal{S}'_{ij}\mathcal{T}'_{ij})\left(\sum_{k=1, k \neq j}^{M_i} \mathcal{K}'_{ik}\widetilde{\mathcal{K}}'^{-1}_{ik} W_{ik} + \sum_{\ell=1, \ell \neq i}^{3} \sum_{k=1}^{M_\ell} \mathcal{K}'_{\ell k}\widetilde{\mathcal{K}}'^{-1}_{\ell k} W_{\ell k} \right) = -u^{\text{in}}, \text{ on } \Gamma^{ij} \tag{3.19}$$

for $j = 1, 2, \ldots, M_i$ and $i = 1, 2, 3$. As in the case of homogeneous media (cf. (2.23)), we find similar equivalence from the above discussions:

$$\mathcal{K}'_{\ell k}\widetilde{\mathcal{K}}'^{-1}_{\ell k} = \widetilde{\mathcal{S}}_{\ell k}, \tag{3.20}$$

and the replacement of the operators $\mathcal{K}'_{\ell k}\widetilde{\mathcal{K}}'^{-1}_{\ell k}$ by the solution operators $\widetilde{\mathcal{S}}_{\ell k}$ can also be applied to (3.19). Then, equations given in (3.19) are rewritten as

$$(\mathcal{I} + \mathbb{K}' - \mathbb{S}'\mathbb{K}')\, \boldsymbol{W} = \boldsymbol{b}, \tag{3.21}$$

where $\boldsymbol{W} = (W_{11}, \ldots, W_{1M_1}, W_{21}, \ldots, W_{2M_2}, W_{31}, \ldots, W_{3M_3})^{\mathrm{T}}$, and

$$\mathbb{S}' = \begin{pmatrix} \mathcal{S}'_{11}\mathcal{T}'_{11} & \cdots & \mathcal{O} \\ \vdots & \ddots & \vdots \\ \mathcal{O} & \cdots & \mathcal{S}'_{3M_3}\mathcal{T}'_{3M_3} \end{pmatrix}, \quad \mathbb{K}' = \begin{pmatrix} \mathcal{O} & \widetilde{\mathcal{S}}_{12} & \cdots & \widetilde{\mathcal{S}}_{3M_3} \\ \widetilde{\mathcal{S}}_{11} & \mathcal{O} & \cdots & \widetilde{\mathcal{S}}_{3M_3} \\ \vdots & \vdots & \ddots & \vdots \\ \dot{\widetilde{\mathcal{S}}}_{11} & \dot{\widetilde{\mathcal{S}}}_{12} & \cdots & \mathcal{O} \end{pmatrix}. \tag{3.22}$$

Now, we apply the GMRES iterative method to solve the system (3.21)–(3.22). We refer to Algorithm 2 for a summary of the algorithm.

Different from the homogeneous media case, we have two types of solution operators $\mathcal{S}'_{ij}$ and $\widetilde{\mathcal{S}}_{\ell k}$ involved in (3.21)–(3.22). For $\mathcal{S}'_{ij}$, we need to solve boundary value problems (3.11), which involve variable refraction index $n(\boldsymbol{x})$. On the other hand, the solution operators $\widetilde{\mathcal{S}}_{\ell k}$ of the exterior problems can also be seen as the extension of the purely outgoing components outside the artificial boundaries Γ^{ij} similar to the homogeneous case. High order discretization for the BVP (3.11) (including (2.26) as a special case) and the solution of the exterior problem (3.2) will be discussed in the next two subsections.

Remark 3.2. Although the boundary data W_{ij} of purely outgoing components w_{ij} on Γ^{ij} are the unknowns in (3.21), the total field $u(\boldsymbol{x})$ in truncated domains $B_{ij} \setminus \Omega_{ij}$ will be calculated in all the iterations.

3.3. High order spectral element discretization for BVPs

Without loss of generality, we take the BVP (3.11) w.r.t a sound soft scatterer Ω_{1j} as an example to show the details of the high order spectral element discretization. Similar spectral element discretization can be extended to other situations straightforwardly. Let $\mathcal{T} = \{K^e\}_{e=1}^{E}$ be a non-overlapping quadrilateral partition of the domain $B_{1j} \setminus \overline{\Omega}_{1j}$ (see Fig. 3.2 (Right)). Assume that each element K^e in the partition $\mathcal{T}$ can be obtained by a transformation $\boldsymbol{F}^e$ from the reference square

$$\widehat{K} = \{\widehat{\boldsymbol{x}} = (\xi, \eta) : -1 \leqslant \xi, \eta \leqslant 1\} = [-1, 1]^2. \tag{3.23}$$

Let

$$\widehat{Q}_p = \text{span}\{\xi^{p_1}\eta^{p_2} : -1 \leqslant \xi, \eta \leqslant 1, 0 \leqslant p_1, p_2 \leqslant p\}, \tag{3.24}$$

be the space of polynomials of degree less than p along each coordinate direction. For any subdomain $K^e \in \mathcal{T}$, we define the finite dimensional space

$$\mathcal{W}_p(K^e) = \{\varphi : \varphi = \widehat{\varphi} \circ (\boldsymbol{F}^e)^{-1}, \; \widehat{\varphi} \in \widehat{Q}_p\}. \tag{3.25}$$

Then the spectral element approximation space is given by

$$\boldsymbol{V}_p = \left\{ v_p \in H^1(B_{1j} \setminus \Omega_{1j}) : v_p\big|_{K^e} \in \mathcal{W}_p(K^e), \; v_p\big|_{\partial\Omega_{1j}} = 0 \right\}. \tag{3.26}$$

Algorithm 2 Iterative algorithm for multiple scattering in locally inhomogeneous media

---

Initialization

(i) Given $\boldsymbol{W}^{(0)}$ on $\{\Gamma^{ij}\}$, stop residue ε and maximum iteration steps n_{max}.

(ii) Solve (3.2) with $g_{ij} = W_{ij}^{(0)}$ for $w_{ij}^{(0)} = \widetilde{\mathscr{S}}_{ij} W_{ij}^{(0)}$ outside B_{ij}, $j = 1, 2, \cdots, M_i$, $i = 1, 2, 3$.

(iii) Solve (3.11) with

$$\psi = \mathscr{T}_{ij}'\left(\sum_{m=1,m\neq j}^{M_i} w_{im}^{(0)} + \sum_{\ell=1,\ell\neq i}^{3} \sum_{m=1}^{M_\ell} w_{\ell m}^{(0)} \right),$$

for the total field $u^{(0)}(\boldsymbol{x}) = \mathscr{S}_{ij}'\psi$ in $B_{ij} \setminus \overline{\Omega}_{ij}$, $j = 1, 2, \cdots, M_i$, $i = 1, 2, 3$.

(iv) Use $w_{ij}^{(0)}$ and $u^{(0)}$ to compute $\boldsymbol{r}^{(0)} = \boldsymbol{b} - (\mathcal{I} + \mathbb{K}' - \mathbb{S}'\mathbb{K}')\boldsymbol{W}^{(0)}$, and $\boldsymbol{v}^{(1)} = \boldsymbol{r}^{(0)}/\|\boldsymbol{r}^{(0)}\|$.

Iterative steps

for $n = 1, 2, \cdots, n_{max}$ **do**

    for $k = 2 \to n$ **do**

        Solve (3.2) with $g_{ij} = v_{ij}^{(k-1)}$ for $w_{ij}^{(k-1)} = \widetilde{\mathscr{S}}_{ij} v_{ij}^{(k-1)}$ outside B_{ij}.

        Solve (3.11) with

$$\psi = \mathscr{T}_{ij}'\left(\sum_{m=1,m\neq j}^{M_i} w_{im}^{(k-1)} + \sum_{\ell=1,\ell\neq i}^{3} \sum_{m=1}^{M_\ell} w_{\ell m}^{(k-1)} \right),$$

        for $\tilde{v}_{ij} = \mathscr{S}_{ij}'\psi$, $j = 1, 2, \cdots, M_i$, $i = 1, 2, 3$.

        Use $w_{ij}^{(k-1)}$ and $\tilde{v}_{ij}$ to compute $\boldsymbol{v}^{(k)} = (\mathcal{I} + \mathbb{K}' - \mathbb{S}'\mathbb{K}')\boldsymbol{v}^{(k-1)}$;

        for $m = 1 \to k - 1$ **do**

$$h_{m,k-1} = (\boldsymbol{v}^{(m)}, \boldsymbol{v}^{(k)}); \quad \boldsymbol{v}^{(k)} = \boldsymbol{v}^{(k)} - h_{m,k-1}\boldsymbol{v}^{(m)}.$$

        end for

        $h_{k,k-1} = \|\boldsymbol{v}^{(k)}\|$, $\boldsymbol{v}^{(k)} = \boldsymbol{v}^{(k)}/h_{k,k-1}$.

    end for

    Compute $W^{(n)} = W^0 + \sum_{i=1}^{n-1} y_i \boldsymbol{v}_i$, where $\boldsymbol{y} = (y_1, y_2, \cdots, y_{n-1})^{\mathrm{T}}$ minimizes

$$J(\boldsymbol{y}) := \big\| \|\boldsymbol{r}_0\|\boldsymbol{e}_1 - \bar{H}_{n-1}\boldsymbol{y} \big\|.$$

    if $J(\boldsymbol{y}) \leq \varepsilon$ **then**

        Stop iteration.

    end if

end for

Final step

Solve (3.2) with $g_{ij} = W_{ij}^{(n)}$ for $w_{ij}^{(n)} = \widetilde{\mathscr{S}}_{ij} W_{ij}^{(n)}$ outside B_{ij}, $j = 1, 2, \cdots, M_i$, $i = 1, 2, 3$.

Solve (3.11) with

$$\psi = \mathscr{T}_{ij}'\left(\sum_{m=1,m\neq j}^{M_i} w_{im}^{(n)} + \sum_{\ell=1,\ell\neq i}^{3} \sum_{m=1}^{M_\ell} w_{\ell m}^{(n)} \right),$$

for total field $u_{ij}^{(n)} = \mathscr{S}_{ij}'\psi$ in $B_{ij} \setminus \overline{\Omega}_{ij}$, $j = 1, 2, \cdots, M_i$, $i = 1, 2, 3$.

The spectral element discretization of (3.11) is to find $v_p \in \boldsymbol{V}_p$ such that

$$\mathcal{A}(v_p, w) = -\langle \mathscr{T}_{1j}' u^{\mathrm{in}} + \psi, w \rangle_{\Gamma^{1j}}, \quad \forall w \in \boldsymbol{V}_p, \tag{3.27}$$

where

$$\mathcal{A}(v_p, w) = -(\nabla v_p, \nabla w)_{B_{1j}\setminus\Omega_{1j}} + \kappa^2(n(\boldsymbol{x})v_p, w)_{B_{1j}\setminus\Omega_{1j}} + \langle \mathscr{T}_{1j} v_p, w \rangle_{\Gamma^{1j}}. \tag{3.28}$$

(a) Curvilinear elements   (b) LGL points on $\widehat{K}$ (c) Mapped LGL points on K^e
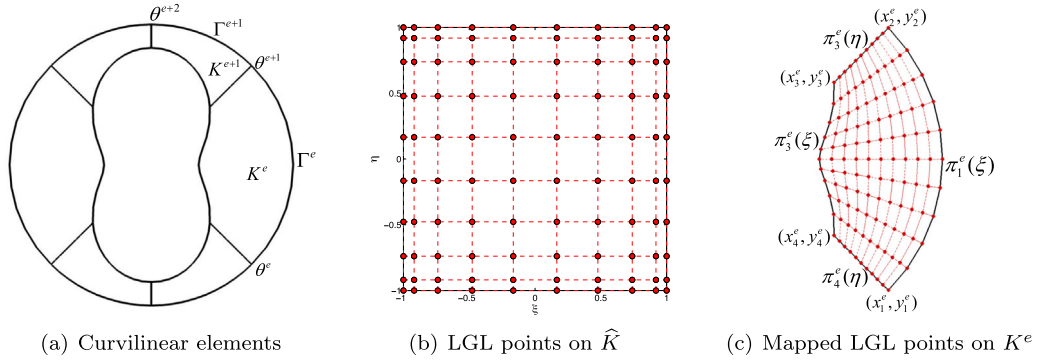
Fig. 3.1. Curvilinear elements and tensorial LGL points on the reference square and a curvilinear element via the new elemental mapping based on Gordon–Hall transformation.

Remark 3.3. In real computation, the DtN boundary condition (2.29) needs to be approximated by the truncation: $\mathscr{T}_{ij}^{N}[v] := \sum_{|n|=0}^{N} \kappa \frac{H_n^{(1)'}(\kappa R_{ij})}{H_n^{(1)}(\kappa R_{ij})} \hat{v}_n e^{in\theta_{ij}}$ with a suitable cut-off number N. Harari and Hughes [31] showed that the choice of $N \geq \kappa R_{ij}$ could guarantee the solvability of the approximate problem with a certified accuracy. We also refer to [32] for the error analysis and numerical studies on the selection of an optimal cut-off number N. In practice, the choice $N \geq \kappa R_{ij}$ is always safe although it is conservative at times. Grote and Keller [33] suggested a different modification of the DtN boundary condition to remove the constraint on κR_{ij} for any fixed N.

In the spectral element discretization, Lagrange nodal basis based on the Legendre–Gauss–Lobatto (LGL) points is used and the continuous inner product $(\cdot, \cdot)_{B_{1j} \setminus \Omega_{1j}}$ can be evaluated by element-wise discrete inner product based on tensorial Legendre–Gauss–Lobatto (LGL) quadrature (see e.g., [34]). However, much care is needed to deal with the term $\langle \mathscr{T}_{1j}^{N} v_p, w \rangle_{\Gamma^{1j}}$, as the DtN operator is global, but the spectral-element approximation is piecewise. One can evaluate by using the fast Fourier transform (FFT), but this requires an intermediate interpolation to interplay between spectral-element grids and Fourier points. Since $v_p|_{\Gamma^{1j}} \in C^0$ a naive interpolation only results in a first-order convergence. Here the semi-analytic means introduced in [35] is adopted to compute $\langle \mathscr{T}_{1j}^{N} v_p, w \rangle_{\Gamma^{1j}}$.

Let us recap on the semi-analytic formula for the computation of $\langle \mathscr{T}_{1j}^{N} v_p, w \rangle_{\Gamma^{ij}}$. Denote by $\{\xi_k = \eta_k\}_{k=0}^{p}$ (in ascending order) the LGL points in $[-1, 1]$, and $\{l_k\}_{k=0}^{p}$ the associated Lagrange interpolating basis polynomials. Correspondingly, the spectral-element grids and basis on K^e are given by

$$\boldsymbol{x}_{k\ell} = \boldsymbol{F}^e(\xi_k, \eta_\ell), \quad \psi_{k\ell}(\boldsymbol{x}) = l_k(\xi)l_\ell(\eta), \quad 0 \leq k, \ell \leq p, \tag{3.29}$$

where $\boldsymbol{F}^e$ is the Gordon–Hall transform [36]. Formally, we can write

$$v_p(x, y)\big|_{K^e} = \sum_{k,\ell} \tilde{v}_{k\ell}^e \, l_k(\xi)l_\ell(\eta), \tag{3.30}$$

where the unknowns $\{\tilde{v}_{k\ell}^e\}$ are determined by the scheme (3.27).

We choose to use the Gordon–Hall transform for the mapping between reference square to our curvilinear element K^e. In particular, we consider a curvilinear element K^e with vertices $\{(x_k^e, y_k^e)\}_{k=1}^{4}$ along Γ^{1j}. Let $\{\boldsymbol{\pi}_k^e(t) = (\pi_{k1}^e(t), \pi_{k2}^e(t)), t \in [-1, 1]\}_{k=1}^{4}$ be, respectively, the parametric form of four sides such that

$$\boldsymbol{\pi}_1^e(-1) = \boldsymbol{\pi}_4^e(1), \quad \boldsymbol{\pi}_1^e(1) = \boldsymbol{\pi}_2^e(1), \quad \boldsymbol{\pi}_2^e(-1) = \boldsymbol{\pi}_3^e(1), \quad \boldsymbol{\pi}_3^e(-1) = \boldsymbol{\pi}_4^e(-1), \tag{3.31}$$

see Fig. 3.1(b). In this case, the Gordon–Hall transform takes the form

$$\begin{aligned}
\boldsymbol{x} = \boldsymbol{F}^e(\xi, \eta) &= \boldsymbol{\pi}_1^e(\xi)\frac{1+\eta}{2} + \boldsymbol{\pi}_3^e(\xi)\frac{1-\eta}{2} + \frac{1+\xi}{2}\boldsymbol{\pi}_2^e(\eta) + \frac{1-\xi}{2}\boldsymbol{\pi}_4^e(\eta) \\
&\quad - \left(\boldsymbol{\pi}_1^e(-1)\frac{1-\xi}{2} + \boldsymbol{\pi}_1^e(1)\frac{1+\xi}{2}\right)\frac{1+\eta}{2} - \left(\boldsymbol{\pi}_3^e(-1)\frac{1-\xi}{2} + \boldsymbol{\pi}_3^e(1)\frac{1+\xi}{2}\right)\frac{1-\eta}{2},
\end{aligned} \tag{3.32}$$

where the edge $\eta = 1$ of $\widehat{K}$ is mapped to the arc $\Gamma^e = \{r = R_{ij}, \ \theta \in (\theta_e, \theta_{e+1})\}$ of K^e, i.e.,

$$\Gamma^e : \quad x = \pi_{11}^e(\xi), \quad y = \pi_{12}^e(\xi), \quad \forall \xi \in [-1, 1]. \tag{3.33}$$

Accordingly, the spectral-element grids in shifted polar coordinates on Γ^e (see Fig. 3.1) satisfy

$$\cos\theta_k^e = R_{1j}^{-1}(\pi_{11}^e(\xi_k) - x_{1j}^c) \ \ \text{or} \ \ \sin\theta_k^e = R_{1j}^{-1}(\pi_{12}^e(\xi_k) - y_{1j}^c), \quad 0 \le k \le p. \tag{3.34}$$

Thanks to (2.29) and (3.30), the calculation of $\langle \mathcal{T}_{ij}^N v_p, w\rangle_{\Gamma^{ij}}$ needs to evaluate

$$\int_0^{2\pi} v_p(x,y)|_{\Gamma^{1j}} e^{-in\theta}\,\mathrm{d}\theta = \sum_{e=1}^{E_\Gamma}\sum_k \tilde{v}_{kp}^e \int_{-1}^1 l_k(\xi) e^{-in\theta(\xi)}\frac{\mathrm{d}\theta}{\mathrm{d}\xi}\,\mathrm{d}\xi, \tag{3.35}$$

where E_Γ is the number of elements which have one edge coincide with Γ^{1j}. As the nodal basis $\{l_k\}$ can be represented in terms of Legendre polynomials, it suffices to compute

$$\mathbb{I}_{nm}^e := \int_{-1}^1 P_m(\xi) e^{-in\theta(\xi)}\frac{\mathrm{d}\theta}{\mathrm{d}\xi}\,\mathrm{d}\xi, \quad \text{for } m \ge 0, \tag{3.36}$$

where P_m is the Legendre polynomial of degree m, and by (3.33),

$$\frac{\mathrm{d}\theta}{\mathrm{d}\xi} = \frac{1}{R_{1j}}\frac{\mathrm{d}\gamma}{\mathrm{d}\xi} = R_{1j}^{-1}\sqrt{[\partial_\xi\pi_{11}^e(\xi)]^2 + [\partial_\xi\pi_{12}^e(\xi)]^2}. \tag{3.37}$$

It is seen that the integrand is highly oscillatory for large $|m|$, and the efficiency and accuracy in computing $\mathbb{I}_{nm}^e$ essentially relies on the choice of the parametric form for $\pi_1^e(\xi)$. It has been shown in [35] that the parametric

$$\pi_1^e(\xi) = (\pi_{11}^e(\xi), \pi_{12}^e(\xi)) = (R_{1j}\cos(\hat{\theta}_e\xi + \beta_e) + x_{1j}^c, R_{1j}\sin(\hat{\theta}_e\xi + \beta_e) - y_{1j}^c), \tag{3.38}$$

with

$$\hat{\theta}_e = \frac{\theta^{e+1} - \theta^e}{2}, \quad \beta_e = \frac{\theta^e + \theta^{e+1}}{2}, \tag{3.39}$$

has a very important property that θ linearly depends on parameter ξ. So the Gordon–Hall transformation (3.32) with parametric (3.38), we have

$$\theta(\xi) = \hat{\theta}_e\xi + \beta_e, \quad \frac{\mathrm{d}\theta}{\mathrm{d}\xi} = \hat{\theta}_e, \tag{3.40}$$

in (3.36). This leads to the following analytic formula (cf. [35]) for the integral (3.36):

$$\mathbb{I}_{n0}^e = 2\hat{\theta}_e\delta_{n0}; \quad \mathbb{I}_{nm}^e = \frac{2\hat{\theta}_e R_{1j}}{i^n}\sqrt{\frac{\pi}{2m\hat{\theta}_e}}J_{n+1/2}(m\hat{\theta}_e)e^{-im\beta_e}, \tag{3.41}$$

and $\mathbb{I}_{n,-m}^e = (\mathbb{I}_{nm}^e)^*$ for $n \ge 0, m \ge 1$, where $J_{n+1/2}$ is the Bessel function of the first kind.

3.4. Computation of the scattering field outside the artificial boundary

Since the purely outgoing wave $w_{\ell k}$ with respect to the scatterer $\Omega_{\ell k}$ will be an incident wave of all other scatterers, we need to compute $w_{\ell k}$ on $\partial\Omega_{ij}$ and Γ_{ij} for multiple scattering problems in homogeneous or locally inhomogeneous media, respectively, in the implementation of the iterative algorithm. We denote by Ω_{ij} another scatterer away from $\Omega_{\ell k}$, and denote by Γ^{ij} another artificial boundary away from $\Gamma^{\ell k}$.

For the homogeneous media case, we can set the artificial boundary $\Gamma^{\ell k}$ used for truncation (2.26) large enough (cf. [21]) to enclose all other scatterers $\{\Omega_{ij}\}$ inside, see Fig. 3.2 (Left) for an example of two scatterers case. In this case, all boundary information on $\partial\Omega_{3j}$ (colored in red) can be obtained via the numerical solution of the BVP (2.26) with respect to Ω_{1j}. However, enclosing all other scatterers leads to a large computational domain and hence high computation cost. It is more efficient to set artificial boundaries close to the scatterers (see Fig. 3.2 (Right)). In fact, the part of the boundary of the scatterer Ω_{3j} (colored in blue) can be inside the domain B_{1j} and the rest part of $\partial\Omega_{3j}$ (colored in red) can be outside B_{1j}. The boundary information w_{1j} on the blue part can be obtained via spectral element solution of the BVP (2.26) with respect to scatterer Ω_{1j}. However, the boundary information on the red part requires an extension of the numerical solution outside B_{1j}. In general, the extension of the spectral element approximation in $B_{\ell k} \setminus \Omega_{\ell k}$ can be obtained by using the values on the artificial boundary $\Gamma^{\ell k}$. Since $\Gamma^{\ell k}$
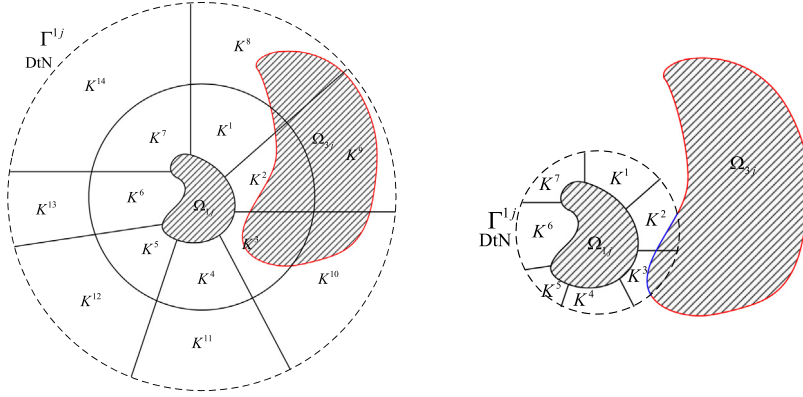
Fig. 3.2. Left: Large artificial boundary to enclose other scatterers. Right: Small artificial boundary intersecting with the boundaries of other scatterers.

here has a circular shape, the extension of a given spectral element solution v_p outside $B_{\ell k}$ is the separation variable solution given by

$$v_p^{\text{ext}}(\boldsymbol{x}) = \sum_{n=-\infty}^{\infty} \frac{\widehat{v}_p^n}{H_h^{(1)}(\kappa R_{\ell k})} H_n^{(1)}(\kappa r_{\ell k}) e^{\text{in}\theta_{\ell k}}, \quad \boldsymbol{x} \notin B_{\ell k}, \tag{3.42}$$

where $(r_{\ell k}, \theta_{\ell k})$ is the polar coordinate of $\boldsymbol{x} - \boldsymbol{c}_{\ell k}$,

$$\widehat{v}_p^n = \frac{1}{2\pi} \int_0^{2\pi} v_p(x_{\ell k}^c + R_{ij} \cos \theta_{\ell k}, y_{\ell k}^c + R_{\ell k} \sin \theta_{\ell k}) e^{-\text{in}\theta_{\ell k}} d\theta_{\ell k}, \tag{3.43}$$

is the Fourier coefficients of $v_p|_{\Gamma^{\ell k}}$. By using the analytic formula (3.41), the Fourier coefficients $\{\widehat{v}_p^n\}$ can be calculated accurately and efficiently for arbitrary high modes.

The scattering problems given by (3.2) will also be solved by using the separation variable method in the same manner due to the circular shape of the artificial boundary $\Gamma^{\ell k}$.

3.5. A comparison with the Grote–Kirsch's approach in [15]

In Grote and Kirsch [15], the reduction of a multiple scattering problem with well separated scatterers using the circular/spherical DtN technique was proposed as an extension of the DtN for a single scattering problem. Consider for example (1.1)–(1.4) with the sound soft scatterers, i.e., $\mathscr{B}_i = \mathcal{I}, i = 1, 2, 3$. The reduced problem therein is to find u and $\{w_j\}_{j=1}^M$ satisfying

$$\begin{cases} \Delta u + \kappa^2 u = 0 & \text{in} \quad B \setminus \bar{\Omega}, \\ u = g, & \text{on} \quad \partial\Omega, \\ \partial_{\boldsymbol{n}} u = \sum_{j=1}^M \mathscr{T}_i[w_j], \quad u = \sum_{j=1}^M \mathscr{P}_i[w_j], & \text{on} \quad \partial B_i, \quad i = 1, 2, \ldots, M, \end{cases} \tag{3.44}$$

where the transport and propagation operators are defined by

$$\mathscr{T}_i[w_i](\theta_i) := \sum_{|n|=0}^{\infty} \widehat{w}_n^i \frac{\kappa H_n^{(1)'}(\kappa R_i)}{H_n^{(1)}(\kappa R_i)} e^{\text{in}\theta_i},$$

$$\mathscr{T}_i[w_j](\theta_i) := \sum_{|n|=0}^{\infty} \widehat{w}_n^j \left(\frac{\kappa H_n^{(1)'}(\kappa r_j(\boldsymbol{x}))}{H_n^{(1)}(\kappa R_j)} \frac{\partial r_j(\boldsymbol{x})}{\partial r_i} + \frac{\text{in} H_n^{(1)}(\kappa r_j(\boldsymbol{x}))}{H_n^{(1)}(\kappa R_j)} \frac{\partial \theta_j(\boldsymbol{x})}{\partial r_i} \right) e^{\text{in}\theta_j(\hat{\boldsymbol{x}})}, \quad j \neq i,$$

$$\mathscr{P}_i[w_i](\theta_i) := w_i(\theta_i) \quad \mathscr{P}_i[w_j](\theta_i) := \sum_{|n|=0}^{\infty} \widehat{w}_n^j \frac{H_n^{(1)}(\kappa r_j(\boldsymbol{x}))}{H_n^{(1)}(\kappa R_j)} e^{\text{in}\theta_j(\boldsymbol{x})}, \quad j \neq i,$$

for $\boldsymbol{x} = (R_i \cos \theta_i + x_i^c, R_i \sin \theta_i + y_i^c) \in \partial B_i$. As mentioned in [15], one can apply any finite-domain solver, e.g., the finite element or spectral element discretization, which typically leads to the linear system:

$$
\begin{pmatrix} \mathbb{K} & \vdots & \mathbb{O} \\ \cdots & \vdots & -\mathbb{T} \\ \mathbb{O} & \mathbb{M} & \vdots & -\mathbb{P} \end{pmatrix} \begin{pmatrix} \boldsymbol{u}_\Omega^h \\ \boldsymbol{u}_{\partial B}^h \\ \boldsymbol{w}^h \end{pmatrix} = \begin{pmatrix} \boldsymbol{g} \\ \boldsymbol{0} \end{pmatrix},
\tag{3.45}
$$

where $\{\boldsymbol{u}_\Omega^h, \boldsymbol{u}_{\partial B}^h\}$ and $\boldsymbol{w}^h$ are the unknowns for the approximation of u and w, respectively. Denote by $\{\Phi_i\}$ and $\mathcal{N} = \mathcal{N}_\Omega \cup \mathcal{N}_{\partial\Omega} \cup \mathcal{N}_{\partial B}$ the nodal basis and nodes used in the discretization. Then the entries of $\mathbb{K}$, $\mathbb{T}$, $\mathbb{M}$, $\mathbb{P}$ and $\boldsymbol{g}$ are given by

$$
\begin{aligned}
K_{ij} &= (\nabla \Phi_j, \nabla \Phi_i)_\Omega - \kappa^2 (\Phi_j, \Phi_i)_\Omega, \quad i, j : \boldsymbol{x}_i, \boldsymbol{x}_j \in \mathcal{N}_\Omega \cup \mathcal{N}_{\partial B}, \\
T_{ij} &= \langle \mathcal{T} \Phi_j, \Phi_i \rangle_{\partial B}, \quad M_{ij} = \langle \Phi_j, \Phi_i \rangle_{\partial B} \quad M_{ij} = \langle \mathcal{P} \Phi_j, \Phi_i \rangle_{\partial B}, \quad i, j : \boldsymbol{x}_i, \boldsymbol{x}_j \in \mathcal{N}_{\partial B}, \\
g_i &= - \sum_{j: \boldsymbol{x}_j \in \mathcal{N}_{\partial\Omega}} g(\boldsymbol{x}_j) K_{ij}, \quad i : \boldsymbol{x}_i \in \mathcal{N}_{\partial\Omega},
\end{aligned}
$$

where the operators $\mathcal{T}$ and $\mathcal{P}$ consist of $\{\mathcal{T}_i\}$ and $\{\mathcal{P}_i\}$. In fact, the matrix $\mathbb{K}$ in (3.45) is block diagonal and the coupling of the scatterers is along the artificial boundary of each scatterer. Indeed, the block iterative method (e.g., block Gauss–Seidel iterative method [23,24]) can be applied.

Although our approach follows the same spirit of "decoupling" the scatterers based on the superposition of waves and suitable iterative solvers, it is different from the existing methods in several aspects. Most importantly, we reduce the multiple scattering problem from a different perspective, which allows us to conduct the convergence analysis and also leads to more efficient algorithm. Indeed, we derive the single scattering problems from the boundary integral theory, and the communications between the scatterers are made simpler through the purely outgoing waves. The use of the GMRES iteration can effectively decouple the interior solver for the single scatterer and interactions from other scatterers (see e.g., Algorithm 2). Through the intrinsic connections between the boundary integral formulation (for the incident waves from other scatterers) and the DtN operator (for the interior solver) on the artificial boundary (cf. (2.23) and (3.19)), we are able to handle the interactions between the scatterers more efficiently and also show the convergence of the iterative approach from the boundary integral theory. In fact, this provides a more flexible numerical framework for multiple scattering problems, and can relax the well separateness assumption of scatterers in [15]. The advantages of our approach are also verified by numerical comparisons with the Grote–Kirsch's approach in Section 5.

4. Convergence analysis for GMRES iteration

In this section, we prove the convergence of the GMRES iteration for (2.24) and (3.21). The key step is to show the compactness of operators $\mathbb{K}$ and $\mathbb{K}' - \mathbb{S}'\mathbb{K}'$. We find it is crucial to use the compactness of the integral operators. In view of the equivalence shown in (2.21) and (2.24); (3.19) and (3.21), we can reformulate $\mathbb{K}$ and $\mathbb{K}'$ in terms of the integral operators. More precisely, we have

$$
\mathbb{K} = \begin{pmatrix} \mathcal{O} & \mathcal{B}_{11} & \cdots & \mathcal{B}_{11} \\ \mathcal{B}_{12} & \mathcal{O} & \cdots & \mathcal{B}_{12} \\ \vdots & \vdots & \ddots & \vdots \\ \mathcal{B}_{3M_3} & \mathcal{B}_{3M_3} & \cdots & \mathcal{O} \end{pmatrix} \begin{pmatrix} \mathcal{K}_{11} \widetilde{\mathcal{K}}_{11}^{-1} & \mathcal{O} & \cdots & \mathcal{O} \\ \mathcal{O} & \mathcal{K}_{12} \widetilde{\mathcal{K}}_{12}^{-1} & \cdots & \mathcal{O} \\ \vdots & \vdots & \ddots & \vdots \\ \mathcal{O} & \mathcal{O} & \cdots & \mathcal{K}_{3M_3} \widetilde{\mathcal{K}}_{3M_3}^{-1} \end{pmatrix},
\tag{4.1}
$$

and

$$
\mathbb{K}' = \begin{pmatrix} \mathcal{O} & \mathcal{K}_{12}' \widetilde{\mathcal{K}}_{12}'^{-1} & \cdots & \mathcal{K}_{3M_3}' \widetilde{\mathcal{K}}_{3M_3}'^{-1} \\ \mathcal{K}_{11}' \widetilde{\mathcal{K}}_{11}'^{-1} & \mathcal{O} & \cdots & \mathcal{K}_{3M_3}' \widetilde{\mathcal{K}}_{3M_3}'^{-1} \\ \vdots & \vdots & \ddots & \vdots \\ \mathcal{K}_{11}' \widetilde{\mathcal{K}}_{11}'^{-1} & \mathcal{K}_{12}' \widetilde{\mathcal{K}}_{12}'^{-1} & \cdots & \mathcal{O} \end{pmatrix}.
\tag{4.2}
$$

We start with reviewing some properties of the usual integral operator defined by

$$
(\mathcal{A}\phi)(\boldsymbol{x}) := \int_G K(\boldsymbol{x}, \boldsymbol{y}) \phi(\boldsymbol{y}) d\boldsymbol{y},
\tag{4.3}
$$

where G is a measurable compact set in $\mathbb{R}^2$. The following conclusion can be found in many text books on linear integral equations (cf. [37,38]).

Theorem 4.2. *If the kernel $K(\boldsymbol{x}, \boldsymbol{y})$ is continuous or weakly singular, then the integral operator $\mathscr{A}$ is a compact operator on $L^2(G)$.*

Theorem 4.3. *Let X be a normed linear space, $\mathscr{A} : X \rightarrow X$ a compact linear operator, and let $\mathcal{I} - \mathscr{A}$ be injective. Then the inverse operator $(\mathcal{I} - \mathscr{A})^{-1}$ exists and is bounded.*

Let us first consider the operator $\mathbb{K}$ involved in homogeneous media case. It consists of the composition of operators $\mathscr{B}_{ij}$, $\mathscr{K}_{\ell k}$ and $\widetilde{\mathscr{K}}_{\ell k}^{-1}$.

Theorem 4.4. *Suppose Ω_{ij} and $\Omega_{\ell k}$ are two different scatterers with C^2 boundary, $\mathscr{B}_{ij}$ are differential operators induced by boundary conditions on $\partial \Omega_{ij}$, $\mathscr{K}_{\ell k}$ are boundary integral operators defined in (2.14). Then the composition $\mathscr{B}_{ij}\mathscr{K}_{\ell k}$ are compact operators from $L^2(\partial \Omega_{\ell k})$ to $L^2(\partial \Omega_{ij})$.*

Proof. From the definition of $\mathscr{B}_{ij}$ and $\mathscr{K}_{\ell k}$, we have

$$(\mathscr{B}_{ij}\mathscr{K}_{\ell k})\phi_{\ell k}(\boldsymbol{x}) = \begin{cases} \mathscr{B}_{ij}\mathcal{D}_{1k}\phi_{1k} + \mathrm{i}\eta\mathscr{B}_{ij}\mathcal{S}_{1k}\phi_{1k} & \ell = 1, \\ -\mathrm{i}\eta\mathscr{B}_{ij}\mathcal{D}_{\ell k}\phi_{\ell k} - \mathscr{B}_{ij}\mathcal{S}_{\ell k}\phi_{\ell k}, & \ell = 2 \text{ or } 3. \end{cases} \tag{4.4}$$

Since $\partial \Omega_{\ell k}$ is a closed curve of class C^2, we have

$$(\mathscr{B}_{ij}\mathcal{S}_{1k})\phi_{1k}(\boldsymbol{x}) = \int_{\partial \Omega_{1k}} \mathscr{B}_{ij}G_\kappa(\boldsymbol{x}, \boldsymbol{y})\phi_{1k}(\boldsymbol{y})dS_{\boldsymbol{y}}, \quad \boldsymbol{x} \in \partial \Omega_{ij},$$

$$(\mathscr{B}_{ij}\mathcal{D}_{1k})\phi_{1k}(\boldsymbol{x}) = \int_{\partial \Omega_{1k}} \mathscr{B}_{ij}\left[\frac{\partial G_\kappa(\boldsymbol{x}, \boldsymbol{y})}{\partial \boldsymbol{n}_{\boldsymbol{y}}}\right]\phi_{1k}(\boldsymbol{y})dS_{\boldsymbol{y}}, \quad \boldsymbol{x} \in \partial \Omega_{ij}. \tag{4.5}$$

Moreover,

$$\begin{cases} \mathscr{B}_{1j}G_\kappa(\boldsymbol{x}, \boldsymbol{y}) = G_\kappa(\boldsymbol{x}, \boldsymbol{y}), \quad \mathscr{B}_{1j}\left[\dfrac{\partial G_\kappa(\boldsymbol{x}, \boldsymbol{y})}{\partial \boldsymbol{n}_{\boldsymbol{y}}}\right] = \dfrac{\partial G_\kappa(\boldsymbol{x}, \boldsymbol{y})}{\partial \boldsymbol{n}_{\boldsymbol{y}}}, \\ \mathscr{B}_{2j}G_\kappa(\boldsymbol{x}, \boldsymbol{y}) = \dfrac{\partial G_\kappa(\boldsymbol{x}, \boldsymbol{y})}{\partial \boldsymbol{n}(\boldsymbol{x})} \quad \mathscr{B}_{2j}\left[\dfrac{\partial G_\kappa(\boldsymbol{x}, \boldsymbol{y})}{\partial \boldsymbol{n}_{\boldsymbol{y}}}\right] = \dfrac{\partial^2 G_\kappa(\boldsymbol{x}, \boldsymbol{y})}{\partial \boldsymbol{n}_{\boldsymbol{x}}\partial \boldsymbol{n}_{\boldsymbol{y}}}, \\ \mathscr{B}_{3j}G_\kappa(\boldsymbol{x}, \boldsymbol{y}) = \dfrac{\partial G_\kappa(\boldsymbol{x}, \boldsymbol{y})}{\partial \boldsymbol{n}(\boldsymbol{x})} + hG_\kappa(\boldsymbol{x}, \boldsymbol{y}), \\ \mathscr{B}_{3j}\left[\dfrac{\partial G_\kappa(\boldsymbol{x}, \boldsymbol{y})}{\partial \boldsymbol{n}_{\boldsymbol{y}}}\right] = \dfrac{\partial^2 G_\kappa(\boldsymbol{x}, \boldsymbol{y})}{\partial \boldsymbol{n}_{\boldsymbol{x}}\partial \boldsymbol{n}_{\boldsymbol{y}}} + h\dfrac{\partial G_\kappa(\boldsymbol{x}, \boldsymbol{y})}{\partial \boldsymbol{n}_{\boldsymbol{y}}}, \end{cases} \tag{4.6}$$

are all continuous for $\boldsymbol{x} \neq \boldsymbol{y}$. By using Theorem 4.2, we conclude that $\mathscr{B}_{ij}\mathcal{D}_{1k}$ and $\mathscr{B}_{ij}\mathcal{S}_{1k}$ are compact operators from $L^2(\partial \Omega_{1k})$ to $L^2(\partial \Omega_{ij})$. Therefore, $\mathscr{B}_{ij}\mathscr{K}_{1k}$ are compact operators from $L^2(\partial \Omega_{1k})$ to $L^2(\partial \Omega_{ij})$. The compactness of operators $\mathscr{B}_{ij}\mathscr{K}_{\ell k} : L^2(\partial \Omega_{\ell k}) \rightarrow L^2(\partial \Omega_{ij})$, $\ell = 2, 3$ can be proved in the same way. $\square$

Note that $\widetilde{\mathscr{K}}_{ij}^{-1}$ are the solution operators of the linear integral equations (2.20). The well-posedness of boundary integral equations (2.20) implies the boundedness of $\widetilde{\mathscr{K}}_{ij}^{-1}$.

Theorem 4.5. *Assume that all boundaries $\partial \Omega_{\ell k}$ is of class C^2, $\mathfrak{Im}(\bar{\kappa}h) \geqslant 0$ and wavenumber κ satisfying $\mathfrak{Im}\kappa \geqslant 0$. Then $\widetilde{\mathscr{K}}_{\ell k}^{-1}$ are bounded linear operators on $L^2(\partial \Omega_{\ell k})$.*

Proof. The boundedness of operator $\widetilde{\mathscr{K}}_{1k}^{-1} : L^2(\partial \Omega_{1k}) \rightarrow L^2(\partial \Omega_{1k})$ is a direct consequence of Theorems 4.2 and 4.3, since

$$\widetilde{\mathscr{K}}_{1k} = \frac{1}{2}\mathcal{I} + \widehat{\mathscr{K}}_{1k} = \frac{1}{2}\mathcal{I} + \widehat{\mathcal{D}}_{1k} + \mathrm{i}\eta\widehat{\mathcal{S}}_{1k},$$

is obviously injective in $L^2(\partial \Omega_{1k})$ and $\widehat{\mathcal{D}}_{1k}$ and $\widehat{\mathcal{S}}_{1k}$ are integral operators with weakly singular kernels.

For operators $\widetilde{\mathscr{K}}_{2k}^{-1}, \widetilde{\mathscr{K}}_{3k}^{-1}$, we need to introduce integral operators

$$\widehat{\mathscr{D}}_{\ell k}^0 \phi_{\ell k}(\boldsymbol{x}) := \text{p.f.} \int_{\partial \Omega_{\ell k}} \frac{\partial^2 G_{\kappa_0}(\boldsymbol{x}, \boldsymbol{y})}{\partial \boldsymbol{n}(\boldsymbol{x}) \partial \boldsymbol{n}(\boldsymbol{y})} \phi_{\ell k}(\boldsymbol{y}) \mathrm{d}S_{\boldsymbol{y}}, \quad \boldsymbol{x} \in \Omega_{\ell k}, \quad \ell = 2, 3, \tag{4.7}$$

where κ_0 is a picked wave number which is not an interior eigenvalue to the corresponding Dirichlet and Neumann problems. An important result is that their inverse $(\widehat{\mathscr{D}}_{\ell k}^0)^{-1}$ exists and are compact on $L^2(\partial \Omega_{\ell k})$ (cf. [37,38]). Then the boundary integral equations (2.20) for $i = 2, 3$ can be transformed into the equivalent forms

$$(\widehat{\mathcal{D}}_{2k}^0)^{-1}\Big(\frac{1}{2}\mathcal{I} - \mathrm{i}\eta(\widehat{\mathcal{D}}_{2k} - \widehat{\mathcal{D}}_{2k}^0) - \widehat{S}_{2k}\Big)\phi_{2k} - \mathrm{i}\eta\phi_{2k} = (\widehat{\mathcal{D}}_{2k}^0)^{-1} W_{2k},$$
$$(\widehat{\mathcal{D}}_{3k}^0)^{-1}\Big(\frac{1 - \mathrm{i}\eta h}{2}\mathcal{I} - \mathrm{i}\eta(\widehat{\mathcal{D}}_{3k} - \widehat{\mathcal{D}}_{3k}^0) - \widehat{S}_{3k}\Big)\phi_{3k} - \mathrm{i}\eta\phi_{3k} = (\widehat{\mathcal{D}}_{3k}^0)^{-1} W_{3k}. \tag{4.8}$$

One can verify that $\widehat{\mathcal{D}}_{\ell k} - \widehat{\mathcal{D}}_{\ell k}^0, \ell = 2, 3$ are integral operators with weakly singular kernels, so they are compact on $L^2(\partial \Omega_{\ell k}), \ell = 2, 3$. Together with the compactness of $(\widehat{\mathscr{D}}_{\ell k}^0)^{-1}$ and $\widehat{S}_{\ell k}$, we conclude that

$$(\widehat{\mathcal{D}}_{2k}^0)^{-1}\Big(\frac{1}{2}\mathcal{I} - \mathrm{i}\eta(\widehat{\mathcal{D}}_{2k} - \widehat{\mathcal{D}}_{2k}^0) - \widehat{S}_{2k}\Big), \quad (\widehat{\mathcal{D}}_{3k}^0)^{-1}\Big(\frac{1 - \mathrm{i}\eta h}{2}\mathcal{I} - \mathrm{i}\eta(\widehat{\mathcal{D}}_{3k} - \widehat{\mathcal{D}}_{3k}^0) - \widehat{S}_{3k}\Big), \tag{4.9}$$

are compact operators on $L^2(\partial \Omega_{\ell k}), \ell = 2, 3$. Then, the boundedness of $\widetilde{\mathscr{K}}_{2k}^{-1}$ and $\widetilde{\mathscr{K}}_{3k}^{-1}$ can be obtained from Theorem 4.3 and the following representations

$$\widetilde{\mathscr{K}}_{2k}^{-1} = \Big[\mathcal{I} - (\mathrm{i}\eta\widehat{\mathcal{D}}_{2k}^0)^{-1}\Big(\frac{1}{2}\mathcal{I} - \mathrm{i}\eta(\widehat{\mathcal{D}}_{2k} - \widehat{\mathcal{D}}_{2k}^0) - \widehat{S}_{2k}\Big)\Big]^{-1} (\mathrm{i}\eta\widehat{\mathcal{D}}_{2k}^0)^{-1},$$
$$\widetilde{\mathscr{K}}_{3k}^{-1} = \Big[\mathcal{I} - (\mathrm{i}\eta\widehat{\mathcal{D}}_{3k}^0)^{-1}\Big(\frac{1 - \mathrm{i}\eta h}{2}\mathcal{I} - \mathrm{i}\eta(\widehat{\mathcal{D}}_{3k} - \widehat{\mathcal{D}}_{3k}^0) - \widehat{S}_{3k}\Big)\Big]^{-1} (\mathrm{i}\eta\widehat{\mathcal{D}}_{3k}^0)^{-1}. \tag{4.10}$$

This ends the proof. $\square$

From Theorems 4.4 and 4.5, we conclude that $\mathscr{B}_{ij}\mathscr{K}_{\ell k}\widetilde{\mathscr{K}}_{\ell k}^{-1}$ are compact operators from $L^2(\partial \Omega_{\ell k})$ to $L^2(\partial \Omega_{ij})$. Now we consider $\mathbb{K}$ which is an operator on the product space

$$\boldsymbol{L}^2(\partial \Omega) := L^2(\partial \Omega_{11}) \times \cdots \times L^2(\partial \Omega_{1M_1}) \times \cdots \times L^2(\partial \Omega_{31}) \times \cdots \times L^2(\partial \Omega_{3M_3}),$$

with the inner product

$$(\boldsymbol{u}, \boldsymbol{v})_{\boldsymbol{L}^2(\partial \Omega)} := \sum_{i=1}^3 \sum_{j=1}^{M_i} (u_{ij}, v_{ij})_{L^2(\partial \Omega_{ij})}, \tag{4.11}$$

and the norm $\|\boldsymbol{u}\|_{\boldsymbol{L}^2(\partial \Omega)}^2 = (\boldsymbol{u}, \boldsymbol{u})_{\boldsymbol{L}^2(\partial \Omega)}$. It is evident that $\boldsymbol{L}^2(\partial \Omega)$ is a Hilbert space.

Theorem 4.6. *The operator $\mathbb{K}$ defined in (2.25) is compact on the Hilbert space $\boldsymbol{L}^2(\partial \Omega)$.*

Proof. For any bounded sequence $\boldsymbol{v}^{(n)} = (v_{11}^{(n)}, \ldots, v_{1M_1}^{(n)}, \ldots, v_{31}^{(n)}, \ldots, v_{3M_3}^{(n)})^{\mathrm{T}}, n = 1, 2, \ldots$, in $\boldsymbol{L}^2(\partial \Omega)$, denote $\tilde{\boldsymbol{v}}^{(n)} = \mathbb{K}\boldsymbol{v}^{(n)}$. Then

$$\tilde{v}_{ij}^{(n)} = \sum_{k=1, k \neq j}^{M_i} \mathscr{B}_{ij}\mathscr{K}_{ik}\widetilde{\mathscr{K}}_{ik}^{-1} v_{ik}^{(n)} + \sum_{\ell=1, \ell \neq k}^3 \sum_{k=1}^{M_\ell} \mathscr{B}_{ij}\mathscr{K}_{\ell k}\widetilde{\mathscr{K}}_{\ell k}^{-1} v_{\ell k}^{(n)}. \tag{4.12}$$

For each scatterer $\Omega_{\ell k}$, $\{v_{\ell k}^{(n)}\}_{n=1}^\infty$ is a bounded sequence in $L^2(\partial \Omega_{\ell k})$ and $\mathscr{B}_{ij}\mathscr{K}_{\ell k}\widetilde{\mathscr{K}}_{\ell k}^{-1}$ are compact operators from $L^2(\partial \Omega_{\ell k})$ to $L^2(\partial \Omega_{ij})$. Thus, each sequence $\{\mathscr{B}_{ij}\mathscr{K}_{\ell k}\widetilde{\mathscr{K}}_{\ell k}^{-1} v_{\ell k}^{(n)}\}_{n=1}^\infty$ in $L^2(\partial \Omega_{ij})$ has a convergent subsequence if Ω_{ij} and $\Omega_{\ell k}$ are different scatterers. Denote the convergent subsequence by $\{v_{ij,\ell k}^{(n)}\}_{n=1}^\infty$. Then the sequence

$$\hat{v}_{ij}^{(n)} = \sum_{k=1, k \neq j}^{M_i} v_{ij,ik}^{(n)} + \sum_{\ell=1, \ell \neq k}^3 \sum_{k=1}^{M_\ell} v_{ij,\ell k}^{(n)}, \quad n = 1, 2, \ldots$$

defined as the finite sum of convergent sequences is a convergent subsequence of $\{\tilde{\boldsymbol{v}}^{(n)}\}_{n=1}^\infty$ in $\boldsymbol{L}^2(\partial \Omega)$. This completes the proof of the compactness of operator $\mathbb{K}$ on $\boldsymbol{L}^2(\partial \Omega)$. $\square$

According to the spectral theorem for compact operator (cf. [39]), $\mathcal{I} + \mathbb{K}$ has a countable sequence of eigenvalues with 1 being the only possible accumulation point. This means the set of eigenvalues λ_j for which $|\lambda_j - 1| > \rho$ for any $\rho < 1$ is finite. Then the convergence of GMRES iteration method for Eq. (2.24) can be concluded from the following result (cf. [40] Proposition 6.1):

Theorem 4.7. *Given a system of linear equations $(I + \mathscr{A})\boldsymbol{w} = \boldsymbol{b}$ where $\mathscr{A}$ is a compact linear operator. Let the eigenvalues of $\mathcal{I} + \mathscr{A}$ be numbered so that $|\lambda_j - 1| \geqslant |\lambda_{j+1} - 1|$, for $j \geqslant 1$. Given $\rho > 0$, determine $0 \leqslant M < \infty$ so that $\{\lambda_j\}_{j=1}^{M} \subset \{z : |z - 1| > \rho\}$, are the outliers and $\{\lambda_j\}_{j \geqslant M+1} \subset \{z : |z - 1| < \rho\}$ is cluster. Define the distance of the outliers from the cluster as*

$$\delta := \max_{|z-1|=\rho} \max_{1 \leqslant j \leqslant M} \frac{|\lambda_j - z|}{|\lambda_j|}.$$

Then for any $\boldsymbol{b}$, and $\boldsymbol{w}_0$

$$\|\boldsymbol{r}_{d+k}\| \leqslant C_\delta \rho^k \|\boldsymbol{r}_0\|,$$

where $\boldsymbol{r}_k$ is the residual generated by GMRES iteration at kth step, and the constant C_δ is independent of k.

Next, we consider the convergence of the proposed iterative method for the multiple scattering problem in locally inhomogeneous media. Following the same proof for homogeneous media case, we can verify that $\mathbb{K}'$ is compact on Hilbert space

$$\boldsymbol{L}^2(\Gamma) := L^2(\Gamma^{11}) \times \cdots \times L^2(\Gamma^{1M_1}) \times \cdots \times L^2(\Gamma^{31}) \times \cdots \times L^2(\Gamma^{3M_3}). \tag{4.13}$$

Therefore, we now focus on the operator $\mathbb{S}'\mathbb{K}'$, which consists of $\mathscr{S}'_{ij}\mathscr{T}'_{ij}\mathscr{K}'_{\ell k}\widetilde{\mathscr{K}}'^{-1}_{\ell k}$.

Lemma 4.1. *Suppose Γ^{ij} and $\Gamma^{\ell k}$ are different artificial boundaries. Then $(\mathscr{K}'_{\ell k}\phi_{\ell k})(\boldsymbol{x}) : L^2(\Gamma^{\ell k}) \to H^{\frac{1}{2}}(\Gamma^{ij})$, $\boldsymbol{x} \in \Gamma^{ij}$ is a compact operator.*

Proof. Let U be a bounded set in $L^2(\Gamma^{\ell k})$, i.e., $\|\phi_{\ell k}\|_{L^2(\Gamma^{\ell k})} \leq C$ for all $\phi_{\ell k} \in U$ and some $C > 0$. Then

$$
\begin{aligned}
|(\mathscr{K}'_{\ell k}\phi_{\ell k})(\boldsymbol{x})| &\leq \int_{\Gamma^{\ell k}} \left| \frac{\partial G_\kappa(\boldsymbol{x}, \boldsymbol{y})}{\partial \boldsymbol{n}(\boldsymbol{y})} \right| |\phi_{\ell k}(\boldsymbol{y})| \mathrm{d}S_{\boldsymbol{y}} + |\eta| \int_{\Gamma^{\ell k}} |G_\kappa(\boldsymbol{x}, \boldsymbol{y})| |\phi_{\ell k}(\boldsymbol{y})| \mathrm{d}S_{\boldsymbol{y}} \\
&\leq C|\Gamma^{\ell k}|^{\frac{1}{2}} \max_{\boldsymbol{y} \in \Gamma^{\ell k}} \left(\left| \frac{\partial G_\kappa(\boldsymbol{x}, \boldsymbol{y})}{\partial \boldsymbol{n}(\boldsymbol{y})} \right| + |\eta| |G_\kappa(\boldsymbol{x}, \boldsymbol{y})| \right),
\end{aligned}
\tag{4.14}
$$

for all $\boldsymbol{x} \in \Gamma^{ij}$ and all $\phi_{\ell k} \in U$, i.e., $\mathscr{K}'_{\ell k} U$ is bounded in maximum norm. Since $\frac{\partial G_\kappa(\boldsymbol{x}, \boldsymbol{y})}{\partial \boldsymbol{n}(\boldsymbol{y})}$ and $G_\kappa(\boldsymbol{x}, \boldsymbol{y})$ are uniformly continuous on the compact set $\Gamma^{ij} \times \Gamma^{\ell k}$, for every $\varepsilon > 0$, there exists $\delta > 0$ such that

$$\left| \frac{\partial G_\kappa(\boldsymbol{x}, \boldsymbol{z})}{\partial \boldsymbol{n}(\boldsymbol{z})} - \frac{\partial G_\kappa(\boldsymbol{y}, \boldsymbol{z})}{\partial \boldsymbol{n}(\boldsymbol{z})} \right| \leq \frac{\varepsilon}{2C|\Gamma^{\ell k}|^{\frac{1}{2}}}, \quad |G_\kappa(\boldsymbol{x}, \boldsymbol{z}) - G_\kappa(\boldsymbol{y}, \boldsymbol{z})| \leq \frac{\varepsilon}{2C|\eta||\Gamma^{\ell k}|^{\frac{1}{2}}}, \tag{4.15}$$

for all $\boldsymbol{x}, \boldsymbol{y} \in \Gamma^{ij}$, $\boldsymbol{z} \in \Gamma^{\ell k}$ with $|\boldsymbol{x} - \boldsymbol{y}| < \delta$. Then

$$|(\mathscr{K}'_{\ell k}\phi_{\ell k})(\boldsymbol{x}) - (\mathscr{K}'_{\ell k}\phi_{\ell k})(\boldsymbol{y})| \leq \varepsilon \tag{4.16}$$

for all $\boldsymbol{x}, \boldsymbol{y} \in \Gamma^{ij}$ with $|\boldsymbol{x} - \boldsymbol{y}| < \delta$ and all $\phi_{\ell k} \in U$, i.e., $\mathscr{K}'_{\ell k} U$ is equicontinuous. By the smoothness of the Green's function $G_\kappa(\boldsymbol{x}, \boldsymbol{y})$ for $\boldsymbol{x} \neq \boldsymbol{y}$, we can further prove that $\{\nabla(\mathscr{K}'_{\ell k}\phi_{\ell k}) : \phi_{\ell k} \in U\}$ is bounded and equicontinuous in the same way. Therefore $(\mathscr{K}'_{\ell k}\phi_{\ell k})(\boldsymbol{x}) : L^2(\Gamma^{\ell k}) \to C^1(\Gamma^{ij})$ are compact. Then the statement of this lemma follows from the facts that $C^1(\Gamma^{ij})$ is dense in $H^{\frac{1}{2}}(\Gamma^{ij})$ and C^1-norm is stronger than $H^{\frac{1}{2}}$-norm. $\square$

Together with the well-posedness of the reduced boundary value problem (3.11), we can draw the conclusion on the compactness of $\mathscr{S}'_{ij}\mathscr{T}'_{ij}\mathscr{K}'_{\ell k}\widetilde{\mathscr{K}}'^{-1}_{\ell k}$.

Theorem 4.8. *Suppose Γ^{ij} and $\Gamma^{\ell k}$ are different artificial boundaries, then*

$$(\mathscr{S}'_{ij}\mathscr{T}'_{ij}\mathscr{K}'_{\ell k}\widetilde{\mathscr{K}}'^{-1}_{\ell k}W_{\ell k})(\boldsymbol{x}) : L^2(\Gamma^{\ell k}) \to H^1(B_{ij} \setminus \Omega_{ij})$$
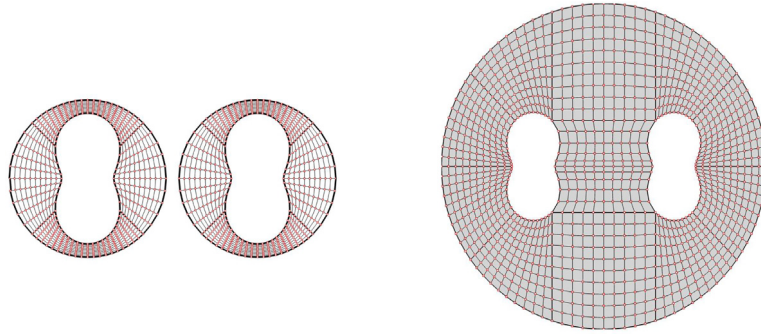
is a compact operator.

Fig. 5.1. Left: Artificial boundaries and spectral element grid for iterative method, Right: Artificial boundary and spectral element grid for reference solution.

Proof. According to the trace theorem in Sobolev space, the DtN operator $\mathscr{T}_{ij}'$ is a bounded linear operator from $H^{\frac{1}{2}}(\Gamma^{ij})$ to $H^{-\frac{1}{2}}(\Gamma^{ij})$ (cf. [30,41]). Moreover, the well-posedness of the boundary value problem (3.11) implies that $\mathscr{S}_{ij}'$ is a bounded operator from $H^{-\frac{1}{2}}(\Gamma^{ij})$ to $H^1(B_{ij} \setminus \Omega_{ij})$. Hence $\mathscr{S}_{ij}' \mathscr{T}_{ij}'$ is bounded from $H^{\frac{1}{2}}(\Gamma^{ij})$ to $H^1(B_{ij} \setminus \Omega_{ij})$.

Note that $\widehat{\mathscr{K}}_{\ell k}'$ is an integral operator with weakly singular kernel, i.e., compact on $L^2(\Gamma^{\ell k})$. By Theorem 4.3, we conclude that $\widetilde{\mathscr{K}}_{\ell k}'^{-1} = \left(\frac{1}{2}\mathcal{I} + \widehat{\mathscr{K}}_{\ell k}'\right)^{-1}$ is a bounded operator on $L^2(\Gamma^{\ell k})$. Together with the boundedness of $\mathscr{S}_{ij}' \mathscr{T}_{ij}'$ in Theorem 3.1 and Lemma 4.1, we complete the proof. $\square$

With the compactness of operators $\mathscr{S}_{ij}' \mathscr{T}_{ij}' \mathscr{K}_{\ell k}' \widetilde{\mathscr{K}}_{\ell k}'^{-1}$, it is not difficult to verify the compactness of $\mathbb{S}'\mathbb{K}'$ on $L^2(\Gamma)$ by following the same proof in Theorem 4.6. Then the convergence of the iterative method for Eq. (3.21) is ensured by Theorem 4.7.

5. Numerical examples

In this section, numerical examples are presented to show the performance of the proposed iterative algorithms. The shape of the scatterers is determined by the parametric form of the boundary curve:

$$r_i = a \sin k(\theta_i - \theta_0) + b, \quad \theta \in [0, 2\pi], \tag{5.1}$$

where (r_i, θ_i) is the polar coordinate of $\boldsymbol{x}$ with respect to a given center $\boldsymbol{c}_i$. In all experiments, we take the plane wave $e^{i\kappa y}$ as the incident wave.

5.1. Homogeneous media

Example 1. We first test the accuracy of Algorithm 1. Consider two scatterers determined by (5.1) with $k = 2$, $a = 0.3$, $b = 0.7$, $\theta_0 = \pi/4$, $\boldsymbol{c}_1(0,0)$ and $\boldsymbol{c}_2(2.6, 0)$. The GMRES iteration is set to stop at the tolerance $1.0\mathrm{e}{-}11$. Since the exact solution is not available, we use the numerical solution computed by spectral element discretization with polynomial of degree $p = 40$ as reference solution u^{ref}. In the computation of the reference solution, we use a large artificial boundary to enclose the two scatterers inside (see Fig. 5.1 (Right)) and impose non-reflecting boundary condition on it. Instead, small artificial boundaries are used for the iterative method, see Fig. 5.1 (Left).

The approximate scattering field with polynomial degree $p = 20$ for the case $\kappa = 20$ is compared with the reference solution in Figs. 5.4 and 5.5. Convergence rates in L^2-norm for cases with wavenumber $\kappa = 10, 20, 30$ are plotted in Fig. 5.2. It shows that the iterative method has spectral accuracy with respect to polynomial degree p. In addition, we plot in Fig. 5.3 the residuals against the number of iterations for different wave number κ and polynomial degree p. Clearly, we see that residuals achieve the machine accuracy in almost the same number of iterations for different polynomial degree $p = 10, 15, 20, 30$. That means the condition number of the iterative method is nearly independent of the degree of freedom used in the spectral element discretization.

To compare with the numerical method proposed in [15], we also adopt the SEM to discretize the truncated problem (3.44) and obtain the linear system (3.45). Then, the GMRES and block GMRES iterative method are
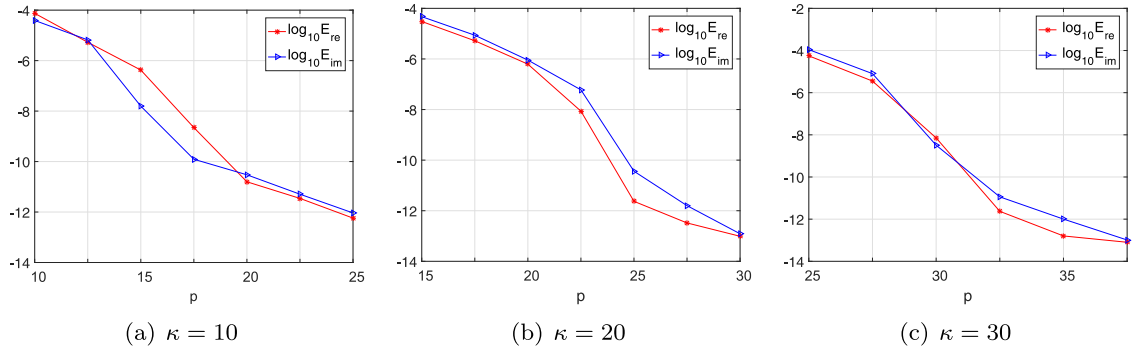
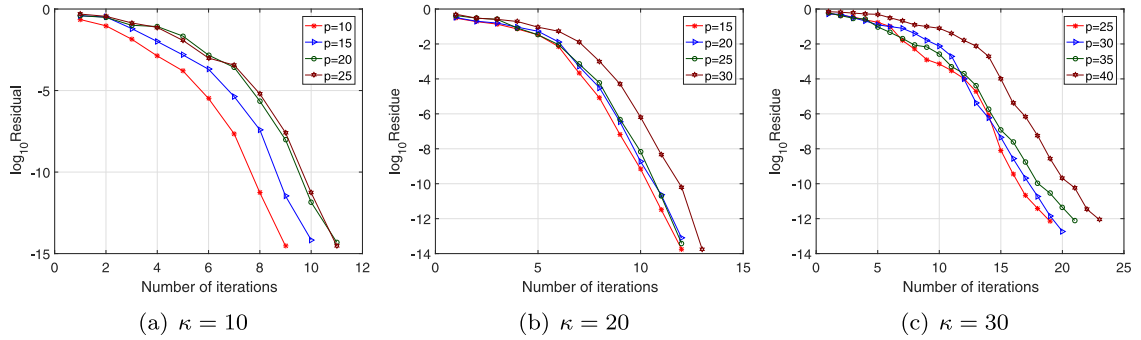Fig. 5.2. Convergence rates in L^2-norm against polynomial degree p.

Fig. 5.3. Residuals against the number of iterations (homogeneous media).
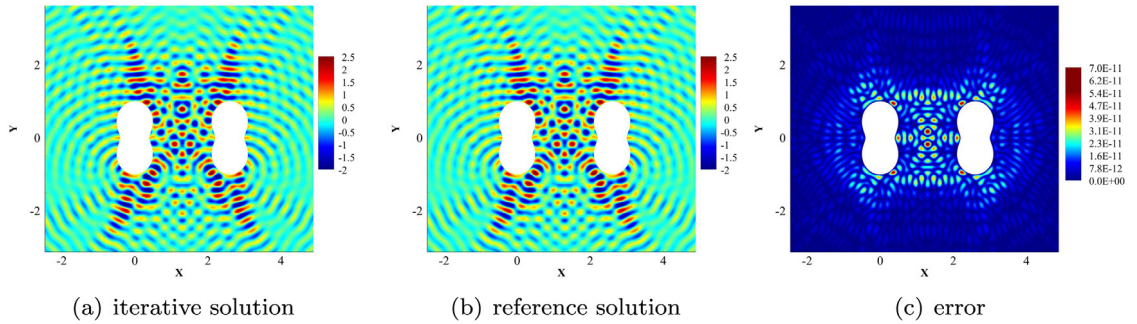

Fig. 5.4. Real parts of iterative numerical solution ($p = 20$), reference solution and error for $\kappa = 20$.

applied to solve it. The iterations are set to stop at residual less than $1.0e-11$. We compare the number of iterations and CPU time required by different methods in Table 5.1. For CPU time comparison, all computations were done on a MacBook Pro with one Intel core i5 2.9 GHz processor and 8 GB RAM. The numerical results show that our iterative method requires fewer iterations and less CPU time than numerical method proposed in [15] combined with block GMRES iterative method for the resulted linear system. This implies that the proposed communication strategy between scatterers in our iterative algorithm is more efficient.

Example 2. As already discussed in Remark 2.1, our iterative method is able to solve the multiple scattering problem with the scatterers being not well-separated. In this example, we consider two scatterers which are close to each other. The parametric expressions of the scatterers are given by (5.1) with $k = 2$, $a = 0.3$, $b = 0.7$, $\theta_0 = \pi/4$. The centers of the scatterers are set to be $c_1(0, 0)$ and $c_2(1.1, 0.5)$. GMRES iteration is set to stop at residual less than

Table 5.1
The number of iterations and CPU time using different numerical methods for multiple scattering problem in homogeneous media.

κ	p	GMRES for (3.45)		Block GMRES for (3.45)		Our iterative algorithm	
		#iterations	Time (s)	#iterations	Time (s)	#iterations	Time (s)
10	10	554	13.8	97	3.4	9	1.8
	15	1400	46.9	106	11.3	10	4.7
	20	2744	118.2	112	39.7	11	12.3
	25	4328	504.7	117	120.9	11	33.6
20	15	1009	45.3	127	13.4	12	5.3
	20	1686	108.8	147	52.7	13	15.7
	25	3807	497.5	153	158.3	13	42.6
	30	5381	862.3	208	397.2	14	112.3

(a) iterative solution

(b) reference solution
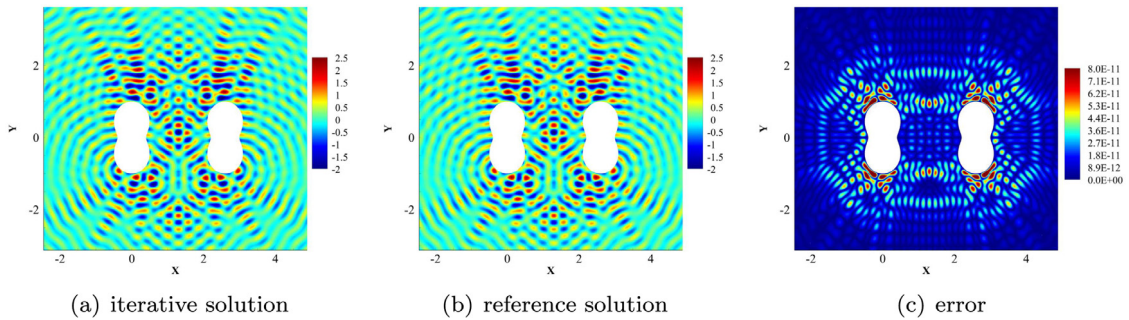
(c) error

Fig. 5.5. Imaginary parts of iterative numerical solution ($p = 20$), reference solution and error for $\kappa = 20$.

(a) 2 not well separated scatterers ($p = 20, \kappa = 20$)

(b) 49 well separated scatterers ($p = 15, \kappa = 10$)
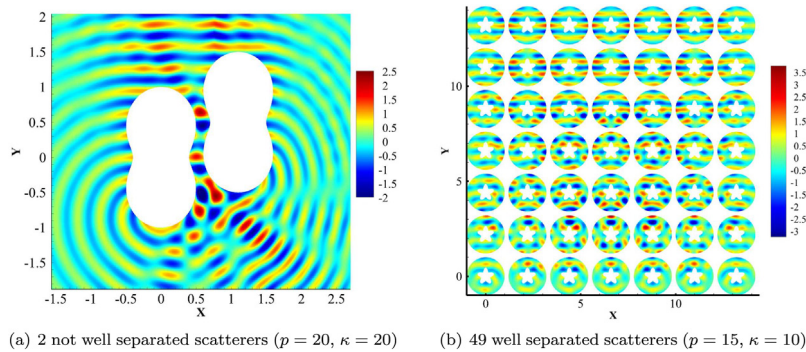
Fig. 5.6. Real parts of the approximate scattering fields due to sound soft scatterers.

1.0e−11. Highly accurate approximation of the real part of the scattering field for the case $\kappa = 20$ is plotted in Fig. 5.6(a).

Example 3. Consider the multiple scattering problem with a large number of scatterers determined by (5.1) with $k = 5, a = 0.2, b = 0.7, \theta_0 = 0$. An array of sound soft (Dirichlet boundary condition) scatterers with centers located at the grid points $\{(2.2n, 2.2m)\}_{n,m=0}^6$ are tested. The real part of approximate scattering field is plotted in Fig. 5.6(b).

Example 4. The scatterers can have different shapes and be randomly distributed. We plot the approximate scattering field due to 16 randomly distributed sound soft scatterers in Fig. 5.7(a). We also test the problem with sound hard (Neumann boundary condition) scatterers, see the approximate scattering field plotted in Fig. 5.7(b).
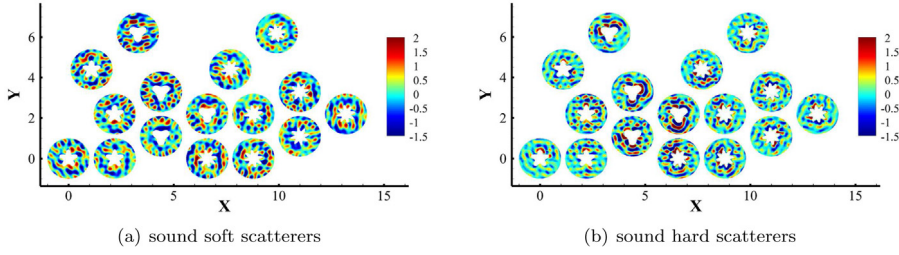
(a) sound soft scatterers

(b) sound hard scatterers

Fig. 5.7. Real parts of the approximate scattering fields ($p = 20$) due to 16 randomly distributed scatterers ($\kappa = 20$).
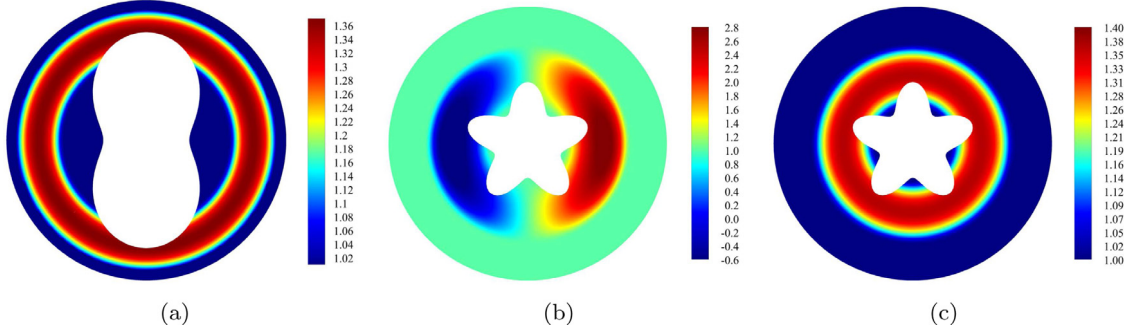

(a)

(b)

(c)

Fig. 5.8. Refraction indices of locally inhomogeneous media.

5.2. Locally inhomogeneous media

Example 5. For accuracy test of Algorithm 2, we consider the same two scatterers problem used in Example 1. All other settings are exactly the same as used in Example 1 except the locally inhomogeneous refraction index

$$n(\boldsymbol{x}) = \begin{cases} \exp(-1/(1 - 16(|\boldsymbol{x} - \boldsymbol{c}_i| - 1)^2)) + 1, & 1.0 < |\boldsymbol{x} - \boldsymbol{c}_i| < 1.25, \\ 1, & \text{otherwise.} \end{cases} \quad (5.2)$$

It is a function of $|\boldsymbol{x} - \boldsymbol{c}_i|$ in the vicinity of the scatterer centered at c_i, see Fig. 5.8(a). L^2-errors of the numerical solutions and corresponding convergence rates are plotted in Fig. 5.9 and an approximate scattering field with $p = 20$ for the case $\kappa = 20$ are compared with reference solution in Fig. 5.10 (real part). Results presented in Fig. 5.9 also show that the iterative method has spectral accuracy. From the decaying rates of residuals plotted in Fig. 5.11, we see that they have similar decaying rates for different polynomial degree $p = 10, 15, 20, 30$ in all tests. Further, the convergence rates of our iterative method and block GMRES iterative method together with numerical discretization proposed in [15] are compared in Table 5.2. All the iterations are set to stop at residual less than 1.0e−11 and the same MacBook Pro is used for CPU time comparison as in Example 1. The comparison results show that our iterative method requires much fewer iterations and accordingly much less CPU time to achieve the given accuracy, which further validates the fact that the way used in our iterative algorithm for the communication between scatterers is more efficient.

Example 6. Set the refraction index

$$n(\boldsymbol{x}) = \begin{cases} x \exp(-1/(1 - 16(|\boldsymbol{x} - \boldsymbol{c}_i| - 0.5)^2)) + 1, & 0.25 < |\boldsymbol{x} - \boldsymbol{c}_i| < 0.75; \\ 1, & \text{otherwise.} \end{cases} \quad (5.3)$$

The contour of $n(\boldsymbol{x})$ is plotted in Fig. 5.8(b). Four scatterers determined by (5.1) with $k = 5, a = 0.3, b = 0.7, \theta_0 = 0$ and centers $(2.2n, 2.2m), n, m = 0, 1$ are considered. The real part of the approximate scattering field is plotted in Fig. 5.12(a). Clearly, we can see stronger scattering in the region which has larger refraction index.
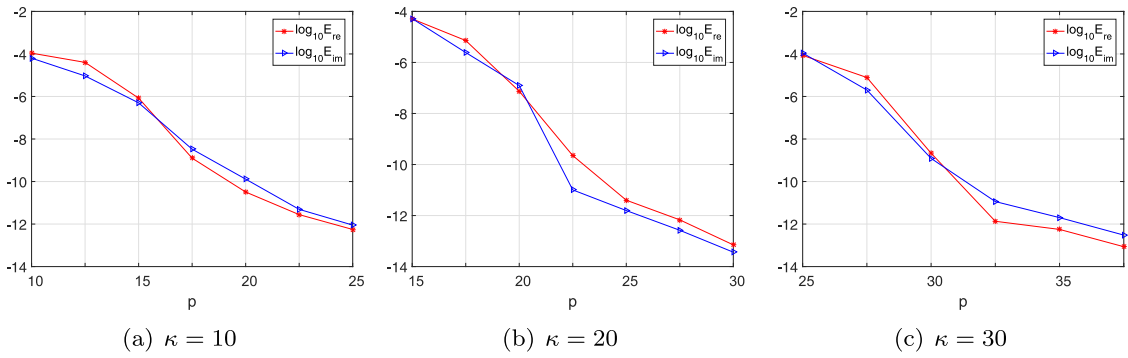
(a) $\kappa = 10$　　　　　(b) $\kappa = 20$　　　　　(c) $\kappa = 30$

Fig. 5.9. L^2-errors against polynomial degree p (inhomogeneous media).

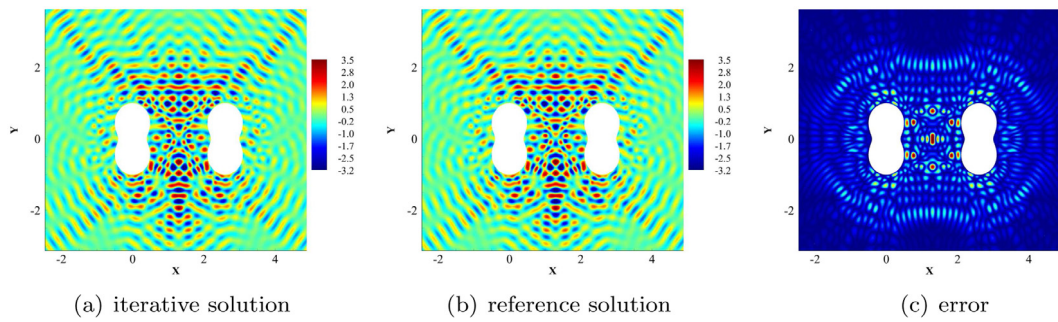(a) iterative solution　　　　(b) reference solution　　　　(c) error

Fig. 5.10. Real parts of iterative numerical solution ($p = 20$), reference solution and error for $\kappa = 20$ and inhomogeneous refraction index given by (5.2).
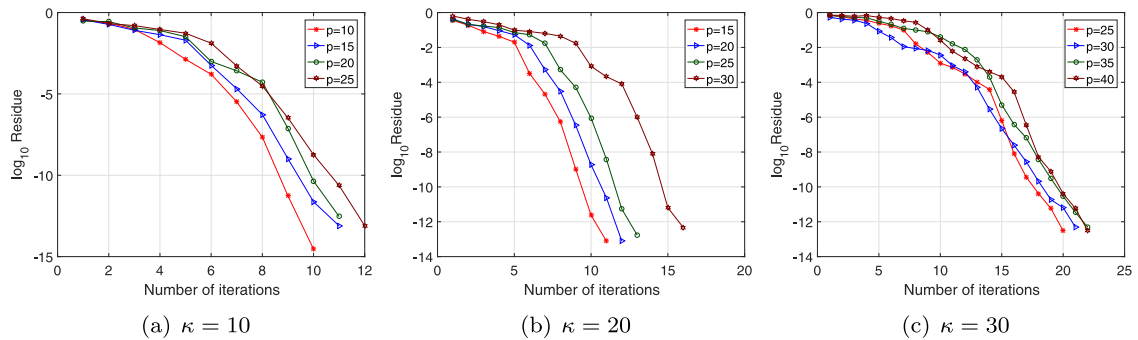

(a) $\kappa = 10$　　　　　(b) $\kappa = 20$　　　　　(c) $\kappa = 30$

Fig. 5.11. Residuals against the number of iterations (inhomogeneous media).

(a) refraction index given by (5.3)　　　　(b) refraction index given by (5.4)
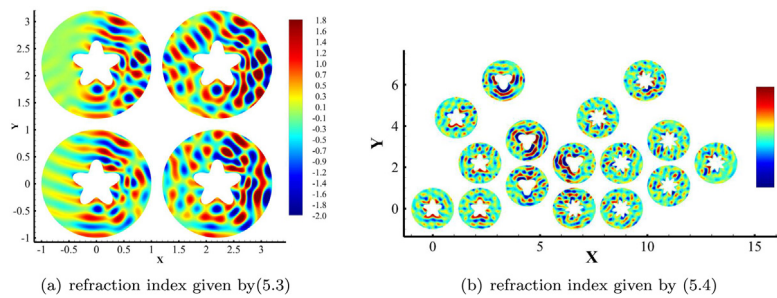
Fig. 5.12. Real parts of approximate scattering fields ($p = 20$) due to 4 and 16 scatterers ($\kappa = 20$).

Table 5.2

The number of iterations and CPU time using different numerical methods for multiple scattering problems in locally inhomogeneous media.

κ	p	GMRES for (3.45)		Block GMRES for (3.45)		Our iterative algorithm	
		#iterations	Time (s)	#iterations	Time (s)	#iterations	Time (s)
10	10	303	8.7	80	2.9	10	1.9
	15	937	35.8	112	13.6	11	5.1
	20	2764	120.1	120	41.6	11	12.8
	25	3978	347.8	126	136.2	12	34.8
20	15	742	32.8	100	10.1	11	4.6
	20	1719	118.7	153	61.3	12	13.4
	25	4021	568.3	166	198.2	14	46.2
	30	5769	923.1	284	489.2	16	121.1

Example 7. Consider the scattering problem with 16 scatterers discussed in Example 3. Set the refraction index

$$n(\boldsymbol{x}) = \begin{cases} \exp(-1/(1 - 16(|\boldsymbol{x} - \boldsymbol{c}_i| - 0.5)^2)) + 1, & 0.25 < |\boldsymbol{x} - \boldsymbol{c}_i| < 0.75; \\ 1, & \text{otherwise}, \end{cases} \tag{5.4}$$

where the contour is plotted in Fig. 5.8(c). The real part of the approximate scattering field is plotted in Fig. 5.12(b).

Conclusion and future work

In this paper, an efficient iterative method for the multiple scattering problem in locally inhomogeneous media is proposed and analyzed. This method is based on boundary integral equations on artificial boundaries. Thus, the iteration converges within a small number of iterations which is nearly independent of the degree of freedom of discretization. At each iteration, only the interior and exterior problems (solved analytically for circular geometry) with respect to single scatterer need to be solved individually. Therefore it has advantages in solving problems with a large number of scatterers. Moreover, it enjoys a great flexibility due to the capability of using various combinations of iterative algorithms and single scattering problem solvers.

For the future work, we will investigate the extension to penetrable scatterers and 3D multiple scattering problems. A preconditioned version for extremely large number of scatterers will also be considered.

Acknowledgments

References

[1] J.W. Young, J.C. Bertrand, Multiple scattering by two cylinders, J. Acoust. Soc. Am. 58 (6) (1975) 1190–1195.
[2] H.A. Ragheb, M. Hamid, Scattering by N parallel conducting circular cylinders, Int. J. Electron. 59 (4) (1985) 407–421.
[3] A.Z. Elsherbeni, A comparative study of two-dimensional multiple scattering techniques, Radio Sci. 29 (04) (1994) 1023–1033.
[4] P. Gabrielli, M. Mercier-Finidori, Acoustic scattering by two spheres: multiple scattering and symmetry considerations, J. Sound Vib. 241 (3) (2001) 423–439.
[5] F.A. Amirkulova, A.N. Norris, Acoustic multiple scattering using recursive algorithms, J. Comput. Phys. 299 (2015) 787–803.
[6] P.A. Martin, Multiple Scattering: Interaction of Time-Harmonic Waves with N Obstacles, Vol. 107, Cambridge University Press, 2006.
[7] D. Colton, R. Kress, Integral Equation Methods in Scattering Theory, SIAM, 2013.
[8] A. Kleefeld, The exterior problem for the Helmholtz equation with mixed boundary conditions in three dimensions, Int. J. Comput. Math. 89 (17) (2012) 2392–2409.

[9] S. Acosta, On-surface radiation condition for multiple scattering of waves, Comput. Methods Appl. Mech. Engrg. 283 (2015) 1296–1309.

[10] P.A. Martin, Integral-equation methods for multiple-scattering problems I. Acoustics, Q. J. Mech. Appl. Math. 38 (1) (1985) 105–118.

[11] M. Ganesh, S.C. Hawkins, An efficient algorithm for simulating scattering by a large number of two dimensional particles, ANZIAM J. 52 (2011) 139–155.

[12] J. Lai, P.J. Li, A fast solver for the elastic scattering of multiple particles, arXiv preprint arXiv:1812.05232.

[13] S.N. Chandler-Wilde, D.P. Hewett, S. Langdon, A. Twigger, A high frequency boundary element method for scattering by a class of nonconvex obstacles, Numer. Math. 129 (4) (2015) 647–689.

[14] A. Gibbs, S.N. Chandler-Wilde, S. Langdon, A. Moiola, A high frequency boundary element method for scattering by a class of multiple obstacles, arXiv preprint arXiv:1903.04449.

[15] M.J. Grote, C. Kirsch, Dirichlet-to-Neumann boundary conditions for multiple scattering problems, J. Comput. Phys. 201 (2) (2004) 630–650.

[16] S. Acosta, V. Villamizar, Coupling of Dirichlet-to-Neumann boundary condition and finite difference methods in curvilinear coordinates for multiple scattering, J. Comput. Phys. 229 (15) (2010) 5498–5517.

[17] S. Acosta, V. Villamizar, B. Malone, The DtN nonreflecting boundary condition for multiple scattering problems in the half-plane, Comput. Methods Appl. Mech. Engrg. 217 (2012) 1–11.

[18] M. Balabane, Boundary decomposition for Helmholtz and Maxwell equations I: disjoint sub-scatterers, Asymptot. Anal. 38 (1) (2004) 1–10.

[19] F. Ecevit, F. Reitich, Analysis of multiple scattering iterations for high-frequency scattering problems. I: The two-dimensional case, Numer. Math. 114 (2) (2009) 271–354.

[20] A. Anand, Y. Boubendir, F. Ecevit, F. Reitich, Analysis of multiple scattering iterations for high-frequency scattering problems. II: The three-dimensional scalar case, Numer. Math. 114 (3) (2010) 373.

[21] C. Geuzaine, A. Vion, R. Gaignaire, P. Dular, An amplitude finite element formulation for multiple-scattering by a collection of convex obstacles, IEEE Trans. Magnet. 46 (8) (2010) 2963–2966.

[22] M. Ganesh, S.C. Hawkins, An efficient $\mathcal{O}(N)$ algorithm for computing $\mathcal{O}(N^2)$ acoustic wave interactions in large N-obstacle three dimensional configurations, BIT 55 (2015) 117–139.

[23] P.J. Li, A.H. Wood, A two-dimensional Helmholtz equation solution for the multiple cavity scattering problem, J. Comput. Phys. 240 (2013) 100–120.

[24] X. Jiang, W.Y. Zheng, Adaptive perfectly matched layer method for multiple scattering problems, Comput. Methods Appl. Mech. Engrg. 201 (2012) 42–52.

[25] X.M. Wu, W.Y. Zheng, An adaptive perfectly matched layer method for multiple cavity scattering problems, Commun. Comput. Phys. 19 (2) (2016) 534–558.

[26] C. Liu, The Helmholtz Equation on Lipschitz Domains, Institute for Mathematics and its Applications (USA), 1995.

[27] G. Verchota, Layer potentials and regularity for the Dirichlet problem for Laplace's equation in Lipschitz domains, J. Funct. Anal. 59 (3) (1984) 572–611.

[28] X. Antoine, C. Chniti, K. Ramdani, On the numerical approximation of high-frequency acoustic multiple scattering problems by circular cylinders, J. Comput. Phys. 227 (3) (2008) 1754–1771.

[29] Y. Saad, M.H. Schultz, GMRES: A generalized minimal residual algorithm for solving nonsymmetric linear systems, SIAM J. Sci. Comput. 7 (3) (1986) 856–869.

[30] J. Melenk, S. Sauter, Convergence analysis for finite element discretizations of the Helmholtz equation with Dirichlet-to-Neumann boundary conditions, Math. Comp. 79 (272) (2010) 1871–1914.

[31] I. Harari, T.J.R. Hughes, Analysis of continuous formulations underlying the computation of time-harmonic acoustics in exterior domains, Comput. Methods Appl. Mech. Engrg. 97 (1) (1992) 103–124.

[32] G.C. Hsiao, N. Nigam, J.E. Pasciak, L.W. Xu, Error analysis of the DtN-FEM for the scattering problem in acoustics via Fourier analysis, J. Comput. Appl. Math. 235 (17) (2011) 4949–4965.

[33] M.J. Grote, J.B. Keller, On nonreflecting boundary conditions, J. Comput. Phys. 122 (2) (1995) 231–243.

[34] M.O. Deville, P.F. Fischer, E.H. Mund, High-Order Methods for Incompressible Fluid Flow, Vol. 9, Cambridge University Press, 2002.

[35] Z.G. Yang, L.L. Wang, Z.J. Rong, B. Wang, B.L. Zhang, Seamless integration of global Dirichlet-to-Neumann boundary condition and spectral elements for transformation electromagnetics, Comput. Methods Appl. Mech. Engrg. 301 (2016) 137–163.

[36] W.J. Gordon, C.A. Hall, Transfinite element methods: blending-function interpolation over arbitrary curved element domains, Numer. Math. 21 (2) (1973) 109–129.

[37] S.G. Mikhlin, Linear Integral Equations, Vol. 2, Delhi, 1960.

[38] R. Kress, V. Maz'ya, V. Kozlov, Linear Integral Equations, Vol. 82, Springer, 1989.

[39] K. Yosida, Functional Analysis, Springer-Verlag, 1978.

[40] S.L. Campbell, I.C. Ipsen, C.T. Kelley, C.D. Meyer, GMRES and the minimal polynomial, BIT 36 (4) (1996) 664–675.

[41] J.-C. Nédélec, Acoustic and Electromagnetic Equations: Integral Representations for Harmonic Problems, Vol. 144, Springer Science & Business Media, 2001.